A study of the Neurodegenerative mechanisms of Alzheimer's and Huntington's Diseases

Nicholas James Parry, BSc



Thesis submitted to the University of Nottingham for the degree of MRes Neuroscience

December 2015

Abstract

Axonal degeneration is a hallmark feature of numerous neurological conditions; one suggested cause of this degeneration is an accumulation of the NAD precursor molecule nicotinamide mononucleotide (NMN), which has been found to signal for cellular apoptosis following axonal injury. Upon treatment with the NAMPT inhibitor FK866 the accumulation of NMN is prevented and axonal survival rate is increased. A similar improvement in axonal survival is shown when nicotinamide mononucleotide adenylyltransferase 2 (NMNAT2), the enzyme responsible for conversion of NMN to NAD is present in excess. Previous studies have indicated that FK866 reduces the occurrence of axonal dystrophies and axonal swellings in Alzheimer's disease (AD) and Huntington's disease (HD) models respectively, my study seeks to expand on these findings by assessing the effect of FK866 on amyloid plaques in AD mice and nuclear aggregates of mutant huntingtin in HD mice, as well as exploring a potential interaction between Huntingtin (Htt) and NMNAT2. No evidence was found to suggest a direct bind between NMNAT2 and Htt, although an indirect interaction cannot be ruled out. My results indicate that while neither medication was found to be effective at reducing amyloid plaque count in the AD model both medication groups showed a reduction in plaque size, potentially accounting for previous findings of a reduced number of axonal dystrophies. It was found that FK866/NA promoted the formation of nuclear aggregates of mHtt in HD model mice while showing no negative cognitive effects, this warrants future study as the role of nuclear aggregates is currently still debated within the literature.

Table of contents

1. Introduction

1.1 Axonal pathology in neurodegenerative disorders p.6-7
- **1.1.1** Wallerian degeneration p.8
- **1.1.2** NMN in regards to disease models p.9

1.2 Alzheimer's disease
- **1.2.1** Disease background p.10
- **1.2.2** Risk factors p.11
- **1.2.3** Proposed mechanisms p.12-16
- **1.2.4** Familial AD and genetic factors p.17-18
- **1.2.5** Differences in onset rate according to gender p.19-21

1.3 Model organisms of Alzheimer's disease p.22-23

1.4 Huntington's disease
- **1.4.1** Disease background p.24
- **1.4.2** Symptoms p.25
- **1.4.3** Aggregates of mutant huntingtin p.26-27
- **1.4.4** Disease mechanism p.28

1.5 Models of Huntington's disease p.29-30

1.6 Memantine and FK866/NA
- **1.6.1** Memantine p.31
- **1.6.2** FK866 p.32

1.7 Aims and objectives p.33

2. Materials and methods

2.1 Mouse origins, breeding and treatment prior to tissue collection p.34
2.2 Cryostat sectioning p.35
2.3 H&E staining p.36
2.4 Immunohistochemistry p.37
2.5 Image acquisition p.38-39
2.6 Data acquisition and analysis p.40
2.7 HEK293T cell cultures p.41
2.8 Transfection of HEK cells p.42
2.9 Preparation of HEK cell whole cell extract p.43

2.10 Transformation of *E.coli* with p-GEX-NMNAT2 p.44
2.11 Protein expression p.45
2.12 Pull down assay p.46
2.13 Co-immunoprecipitation of NMNAT2 and HTTQ23 p.47
2.14 SDS-PAGE p.48
2.15 Western blot p.49
2.16 Preparation of superior cervical ganglia dissociated cells p.50
2.17 Microinjection of SCG cells p.51

3. Results

3.1 Neither memantine or FK866/NA were found to significantly reduce plaque count in the APPswe/PS1ΔE9 mouse model p.52-57

3.2 Both treatment groups were shown to have reduced plaque sizes compared to the vehicle control group p.58-59

3.3 Average plaque area was found to be reduced in both treatment groups p.60-62

3.4 Fk866/NA was shown to increase the rate of formation of nuclear aggregates of mHtt p.63-68

3.5 Pull down assay results of NMNAT2 and Htt show no evidence of a direct bind p.69-71

3.6 Co-immunoprecipitation confirms no direct bind occurs between NMNAT2 and Htt p.72-73

3.7 NMNAT2 and Htt found to be transported separately along the axon p.74-75

4. Discussion p.76

4.1 Medications were found to have no effect on plaque count, average plaque size was found to be reduced p.77-78

4.2 No direct correlation was found between dystrophies and plaque count p.79

4.3 Consistent differences were found between male and female mice in the AD model p.80

4.4 FK866/NA was found to consistently increase the formation of nuclear aggregates of mHtt p.81-83

4.5 A direct bind between NMNAT2 and Htt was found to be unlikely p.84-85

4.6 A potential alternative to the multiple t-test p.86

5. Conclusions p.87

6. Acknowledgements p.88
7. Appendices p.89-90

8. Bibliography p.91-99

Figures

1 NAD synthesis pathway p.7
2 Effect of FK866/NA on dystrophy count p.14
3 Proposed models of Alzheimer's disease pathology p.16
4 AD gender difference p.21
5 Brain analysis regions p.39
6 Average plaque count p.53
7 Plaque and dystrophy colocalisation p.55
8 Average plaque count per cortex region p.57
9 Plaque size groupings p.59
10 Average plaque areas p.61-62
11 mHtt aggregation p.64-67
12 Pull down assay analysis p.70-71
13 Co-immunoprecipitation analysis p.73
14 Microscopy results of axonal transport of NMNAT2 and Htt p.75
15 Behavioural studies of Q140 and APPswe mice p.82

Tables

1 AD genetic factors p.18

Introduction

1.1 Axonal pathology in neurodegenerative disorders

One of the key areas of focus in this study is the role of NMN in the neurodegenerative process of both Huntington's disease (HD) and Alzheimer's disease (AD). NMN is an intermediate of the NAD synthesis pathway (see figure 1) whose formation is catalysed by the enzyme NAMPT and then scavenged by the proposed neuronal survival factor nicotinamide mononucleotide adenylyltransferase 2 (NMNAT2) to form NAD. NMNAT2 belongs to the NMNAT family of enzymes, each involved in the biosynthesis of NAD (Ljungberg, Ali et al. 2011) though differing in location within the cell, NMNAT1, NMNAT2 and NMNAT3 being nuclear, cytosolic and mitochondrial respectively. It is NMNAT2 that is of particular interest due to evidence of its neuroprotective properties (Ljungberg, Ali et al. 2011) as well as its potential involvement in disrupted axonal transport in neurodegenerative disorders. Both AD and HD have documented evidence of impaired axonal transport, with the accumulation of mHtt forming aggregates and potentially blocking axonal transport in HD (Lee, Yoshihara et al. 2004), and the implications that mutated presenilin 1, a genetic factor documented to play a role in AD, causing an impairment to kinesin based axonal transport (Pigino, Morfini et al. 2003). Neurons are particularly prone to complications due to impaired axonal transport due to their structure, typically possessing long, branched axons and dendrites and extending over distances far surpassing other cells, maintaining axon integrity is vital both to the function and survivability of the cell (Stokin and Goldstein 2006). A previous study (Di Stefano, Nascimento-Ferreira et al. 2015) has shown that an accumulation of NMN within the distal axon induces axon degeneration after an injury. Therefore FK866, an inhibitor of NAMPT, blocks axonal degeneration by limiting the NMN levels. Its effect is comparable to that conferred by the expression of the Wallerian degeneration slow (WLD^S) gene (Samsam, Mi et al. 2003) (Beirowski, Babetto et al. 2008), both of which appear to limit the rate of axonal degeneration by delaying the accumulation of NMN. In the case of (Di Stefano, Nascimento-Ferreira et al. 2015) this was demonstrated by a cut to the distal end of neurites, followed by no treatment, the addition of FK866, or the addition of both FK866 and NMN in 3 separate groups. Untreated neurites underwent degeneration, while the FK866 treated cells were still intact, indicating a protective effect conferred by FK866. Interestingly upon treatment with both FK866 and NMN the cells resembled the untreated group, with neurodegeneration apparent in all cells. This would suggest that the neuroprotective effect is not a direct cause of the FK866, rather by

the inhibition of NMN formation, as exogenous NMN may still cause degeneration.

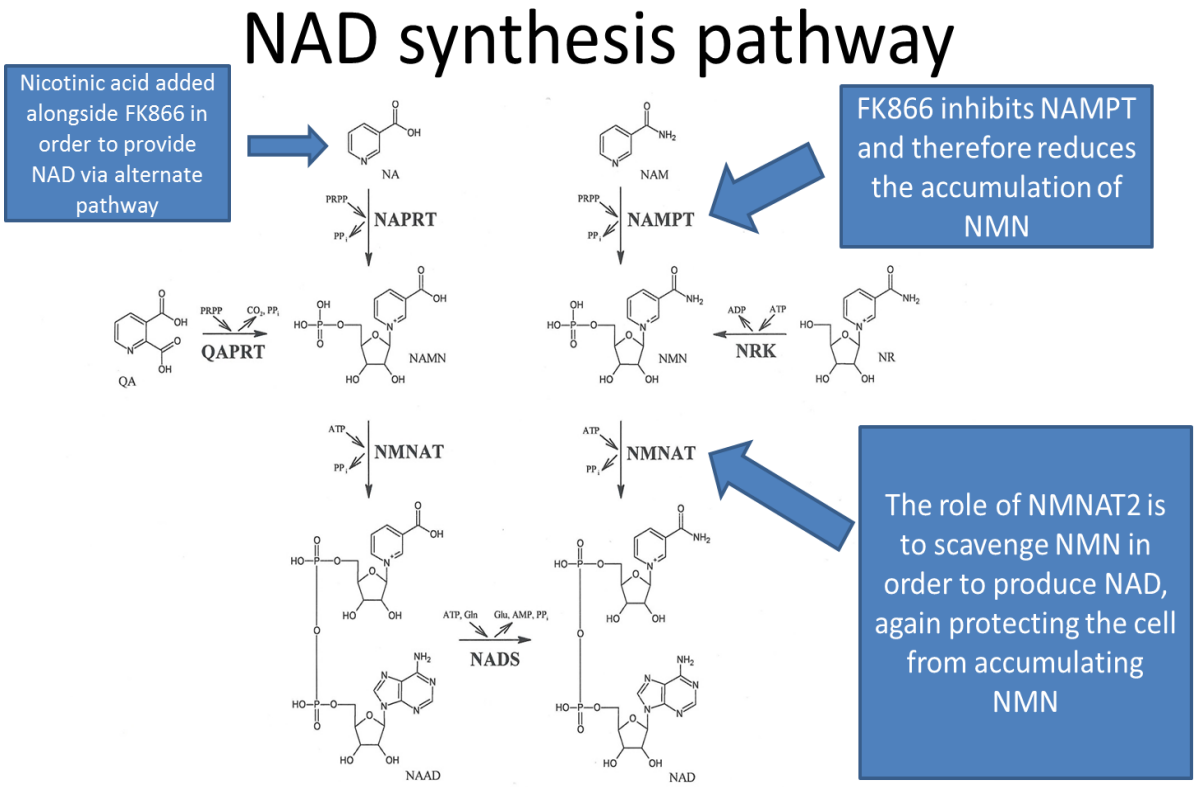


Figure 1. NAD synthesis pathway

As illustrated in the figure one of the primary focuses of the study is the role of NMN and its mechanism in signalling apoptosis as shown in the study (Di Stefano, Nascimento-Ferreira et al. 2015).
Inhibition of NMN was shown to prevent the production of NAD and so nicotinic acid was added alongside FK866 to allow for NAD to be produced via a separate pathway.

1.1.1 Wallerian degeneration

In order to understand the potential significance that NMNAT2 as a neuronal survival factor may play in Huntington toxicity it is first important to have an understanding of the process of wallerian degeneration. Defined as the process by which an axon degenerates distal to an injury, a similar effect is also observed in the case of impaired axonal transport, particularly in some neurodegenerative disorders. Due to the similarities between the mechanisms of Wallerian degeneration and neurodegeneration in a number of diseases the discovery of the Wallerian degenerateion slow (WLD^S) gene was an important breakthrough in the understanding of Axonal degeneration (Conforti, Gilley et al. 2014). The WLD^S gene is an autosomal dominant mutation and was found to delay axonal degeneration from the usual period of around 24 hours to around 3 weeks (Coleman, Conforti et al. 1998), such a significant degree of protection could not be replicated by the addition of either NMNAT1 or NAD^+ (Conforti, Fang et al. 2006). More recent work has suggested that the mechanism by which both NMNAT and WLD^S function is not by fuelling the production of NAD^+, rather by limiting the accumulation of NMN (Di Stefano, Nascimento-Ferreira et al. 2015) which has been implicated to hasten the process of axonal degeneration. Much like cellular apoptosis, the process by which axons degenerate is regulated, and is highly conserved (Adalbert, Gillingwater et al. 2005) throughout numerous species including mice, rats, and humans.

1.1.2 NMN in regards to disease models

With NMN assumed to play a key role in neuronal degeneration and with its only known function being an intermediate molecule in the synthesis of NAD it became of great interest to study any factors capable of reducing or preventing the formation of NMN in the context of a disease model. With NMNAT2 shown to confer neuroprotection (Conforti, Gilley et al. 2014) through the scavenging of NMN, it became one of the main focuses of my study after the apparent co-localisation with Htt in the Golgi apparatus. Due to the short half-life of NMNAT2 (Gilley and Coleman 2010) its consistent transport to the distal end of the axon is required to prevent the build-up of NMN and to ensure a constant supply of NAD, thus in HD where axonal transport has been shown to be impaired (Shirendeb, Calkins et al. 2012) a reduction in the transport of NMNAT2 to the distal ends of the axon may mimic the effects of cut axons documented in (Di Stefano, Nascimento-Ferreira et al. 2015). To further reinforce this hypothesis, previous behavioural studies in our lab conducted on the Q140 mice whose brains are utilised in my analysis of nuclear aggregates of Htt, revealed that upon treatment with FK866/NA there was a statistically significant reduction of axonal swellings present in the striatum, as well as clear signs of cognitive improvement compared to untreated Q140 mice demonstrated via rotarod and prepulse inhibition trials. Note that in the *in vivo* studies Nicotinic acid (NA) has been added alongside FK866 in order to provide a separate pathway through which to produce NAD (see figure 1). Studies conducted on SCG cells typically saw the neurites degenerating over a period of 24 hours, thus the depletion of NAD was less of a deciding factor as typically longer periods are required for cell death to occur as a result of a lack of NAD (Del Nagro, Xiao et al. 2014) (Alano, Garnier et al. 2010). In the case of our Q140 mice whose treatment with FK866 occurred over the course of two weeks nicotinic acid was added to the treatment in order to rule out any effects of the treatment being due to NAD depletion.

1.2 Alzheimer's Disease

1.2.1 Disease background

Due to the advances in modern medicine life expectancies are on the rise across the globe, it is now common for people of first world countries to live to the age of 80. As a result of this we are seeing a rise of degenerative diseases that correlate with old age. Particularly common is the instance of dementia among the elderly population, which as of March 2015 is stated by the World Health Organisation (WHO) to affect 47.5 million people worldwide. Constituting nearly 70% of these cases of dementia (Burns and Iliffe 2009) are those suffering from Alzheimer's disease (AD), a neurodegenerative condition that in its sporadic form accounts for a vast number of dementia cases in those over 65. Alzheimer's disease is a chronic neurodegenerative condition that at the current time has no known cure, in its early stages the disease is characterised by short term memory loss (Burns and Iliffe 2009). Life expectancy following a diagnosis of late onset Alzheimer's disease is between 3 and 9 years (Querfurth and LaFerla 2010, Todd, Barr et al. 2013) (Todd, Barr et al. 2013) with symptoms progressing from short term memory loss to more severe cognitive effects such as mood swings and disorientation, eventually the sufferer is no longer able to live independently and may require full time care. Typically the cause of death is an external factor, with pneumonia commonly recorded as the cause of death with those found to be in the late stages of the disease (Kukull, Brenner et al. 1994), it is thought that due to cognitive impairment AD patients may be less likely to notice the symptoms of other diseases and so both diagnosis and treatment are hindered, thus increasing the likelihood of external health factors causing complications .

1.2.2 Risk factors

Due to the world's ever increasing population and a total of 7.7 million (WHO figure) new diagnoses of dementia a year neurodegenerative disorders are to become ever more problematic, both in terms of healthcare and financially. In the case of late stage AD the patient may require permanent care to be provided, as cognitive function can potentially decline to the point that even simple tasks can become complicated. This care may either be provided by the family or provided via the healthcare system, in some cases through residential nursing homes or in more extreme cases hospital care. In first world countries it is typical that the ratio of the retired population compared to those of working age is consistently shifting towards the retired, thus a socio-economic strain is placed on those of working age and their respective countries to fund the care of an increasing number of AD patients. It is therefore of great importance to develop new strategies of both prevention, and treatment of the disease as the correlation with age would dictate that as life expectancy increases so too does the number of cases of AD. The form of AD occurring over the age of 65 is referred to as late onset Alzheimer's disease (LOAD). Typically the causes of LOAD are more varied and difficult to account for, incorporating both environmental and genetic risk factors, however the primary risk factor contributing to LOAD is age, with studies suggesting a susceptibility to the disease increasing as high as 14 fold above the age of 85 compared to those between the ages of 65 to 69 (Hebert, Scherr et al. 1995).

A number of factors may contribute to this, from oxidative damage over the course of a lifetime, to reduced ability to degrade Aβ due to down regulation of Aβ degrading enzymes such as neprilysin leading to the formation of amyloid plaques. It is clear that the correlation of AD with age is significant, the US census for the year 2000 estimated the incidence of AD in the over 84 group to be as high as 42%, with such a high percentage of the population affected it may be the case that neurodegeneration in the form of dementia is simply a biological inevitability. This may only be determined as lifespans continue to increase and data is accumulated to account for older age groups, if the correlation of Alzheimer's onset with age continues along the same trend it would affect the majority of the population in those age groups above the previously stated 84 years and above. In this regard it may be the case that while neurodegeneration via AD may be inevitable, certain genetic and environmental factors may delay its onset so as to never appear within a person's lifetime.

1.2.3 Proposed mechanisms

With this in mind it is of vital importance to improve our understanding of the condition and to address its underlying mechanisms since current treatment methods focus on symptom management rather than prevention. Sporadic AD is the more common variant of the disease; as such it is quite difficult to predict who amongst the population is more prone to the disorder. Often the early stage symptoms will go unnoticed and so treatment may only begin once more severe cognitive decline becomes noticeable, at which point neuronal loss may already be significant. As of yet there is no way to replace neurons that are lost or damaged, thus symptoms are not reversible and so symptom management and treatment to prevent further decline is all that is available. Ideally in order to effectively manage and treat the disease it must be diagnosed in its very early stages.

A widely used hypothesis regarding the mechanisms behind AD pathology is the Amyloid hypothesis. This suggests that the predominant causative factor in Alzheimer's pathology is the deposition of amyloid plaques (Karran, Mercken et al. 2011). Studies suggest that formation of plaques leads to neurons becoming dystrophic (Meyer-Luehmann, Spires-Jones et al. 2008) (see figure 2) eventually leading to axonal degeneration. The support for this hypothesis largely comes from genetic models of the disease, with mutations to the APOE gene reducing the ability to clear Aβ and thus leading to earlier onset of disease symptoms, consistent with this other genetic alterations to genes related to the Aβ protein also confer Amyloid disease symptoms in model organisms. For example mouse models transgenically expressing the mutated human APP protein also develop AD symptoms (Kokjohn and Roher 2009), in the case of my study the APPswe/PS1ΔE9 has been utilised, developing amyloid plaques along with cognitive deficits at the age of 6 months. Also of interest is the location of the gene coding for the APP protein, as it is located on chromosome 21 in humans an additional copy of the gene is present in the instance of trisomy 21. A study by Nistor *et al* (Nistor, Don et al. 2007) demonstrated that the extra copy of the APP coding region amplified its effect and produced an excess of Aβ, thus conferring AD symptoms, it is common in Down's syndrome patients that AD symptoms occur by the age of 40 and so supporting the hypothesis and implication that the APP protein plays a role in AD pathology. The addition of an extra gene coding for the APP protein is consistent with the proposed mechanism of plaque formation, as an excess of the APP protein, once cleaved by β or γ secretases would lead to an accumulation of Aβ, in particular an excess of the more fibrillary Aβ42, which has been associated with AD. This leads to the aggregation of Aβ eventually leading to

amyloid plaques around the neurons. However, more recent studies have indicated that the rate of amyloid deposition in the brains of AD patients and the onset of Alzheimer's symptoms are not linear (Price, McKeel et al. 2009), this alongside the fact that most medications focused on Aβ show no improvements with regard to cognitive decline (Golde, Petrucelli et al. 2010) indicates that the amyloid hypothesis may only represent a part of the underlying mechanisms of the disease, and is not necessarily the sole causative factor.

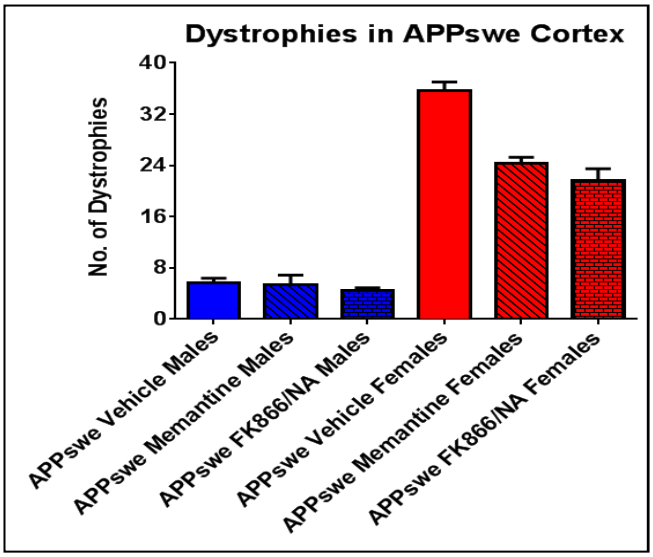


Figure 2. Effect of FK866/NA on dystrophy count
Dystrophy count was analysed during previous work within the lab, data was gathered via confocal microscopy using a 10x air objective and the final dystrophy number expressed as dystrophies per cortex. Dystrophy count was found to be reduced in females by both memantine, a medication already in use for the treatment of AD, as well as FK866/NA, previously implicated as protective against neuronal degeneration following acute injuries (O.Othman, unpublished thesis 2015).

An alternative to the amyloid hypothesis is that of tau hyperphosphorylation, this hypothesis implies that AD pathology may at least partially be explained by the phosphorylation, and subsequent aggregation and tangling of Tau protein fibres within the neuron (Small and Duff 2008). This may potentially cause structural alterations to the cytoskeleton, as well as impaired axonal transport, the effects of which include inhibited signalling between neurons, and eventually could lead to cell. Evidence of this hypothesis does not seem to support tau hyperphosphorylation as the sole cause of AD, with a study of thirteen families all of which were positive for an autosomal dominantly inherited dementia called frontotemporal dementia and Parkinsonism linked to chromosome 17 (FTDP-17) (Hutton, Lendon et al. 1998) revealing that the mutations causing the dementia were present in the same region of chromosome 17 as the gene coding for tau. Three mutations were identified in the 5' splice site of exon 10, proposed to be involved in the regulation of alternative splicing of exon 10 (Goedert, Spillantini et al. 1989). Up-regulation of the splicing of exon 10 was found to increase the proportion of tau protein containing four microtubule binding repeats and through microtubule destabilisation increase the amount of unbound tau capable of forming the pathogenic fibrils seen in AD cases. The implication of this is that while dysfunctional tau proteins may be capable of inducing dementia, it does not cause AD. While it clearly plays a role in AD as tau fibrils are synonymous with the disease, tau hyperphosphorylation alone does not account for the full disease mechanism. With regards to Figure three this may imply the likelihood of the dual pathway model as dysfunctional tau protein may potentially be present without the influence of Aβ. This model may also explain why the results of studies focusing purely on the reduction of Aβ do not show significant cognitive improvements, whereas in the Serial model, in which amyloid pathology is a pre-requisite of tau phosphorylation, it would be expected that a reduction of Aβ would entirely halt AD pathology as the reduction in Aβ would also prevent the accumulation of phosphorylated tau proteins(see Figure 3).

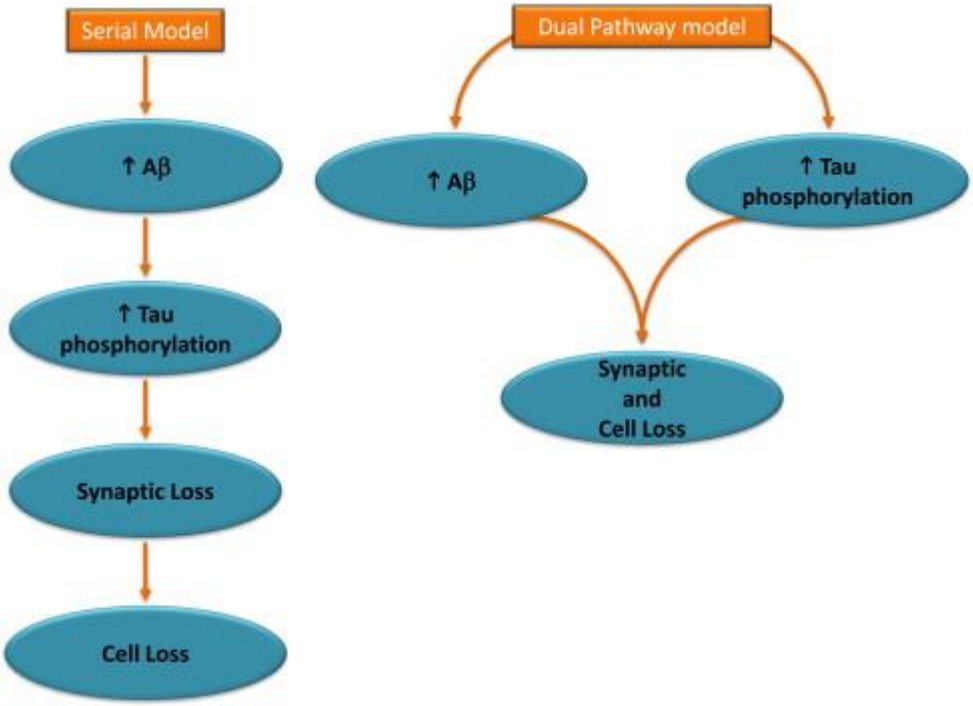


Figure 3. Proposed models of Alzheimer's disease pathology

The serial model suggests a cascade brought about by increased levels of Aβ, with this being the cause of excess phosphorylation of Tau and thus leading to neurodegeneration. Alternatives to this theory have proposed that Tau phosphorylation occurs independently, as shown by its isolated ability to cause other forms of dementia (Hutton, Lendon et al. 1998). The combination of increased Aβ and the increased levels of phosphorylated Tau possibly leading to AD pathology due to the accumulation of both amyloid plaques as well as neurofibrillary tangles caused by hyperphosphorylation of tau proteins.

Image sourced from (Small and Duff 2008)

1.2.4 Familial AD and genetic factors

Far less common than LOAD is Familial Alzheimer's disease, or early onset Alzheimer's disease (EOAD) which is often the result of mutations to genes, commonly genes involved with the production of Aβ (Chartier-Harlin, Crawford et al. 1991). One of the most well-known genetic factors suggested to be present in 40%-80% of Alzheimer's patients (Mahley, Weisgraber et al. 2006) (Strittmatter, Saunders et al. 1993) is the ε4 allele of the Apilipoprotein E (APOE) gene. ApoE4 undergoes a unique proteolysis that does not occur in other variants of the protein, these fragments are documented to be toxic to the cell and can cause cytoskeletal alterations, disruption of the mitochondrial energy balance and eventually cell death (Mahley, Weisgraber et al. 2006). ApoE is produced by the cell in response to stress or damage to the central nervous system (CNS), in the case of those positive for the ApoE4 allele this may result in the toxic effects of proteolytic fragments of ApoE4 being exacerbated. It has been implicated that ApoE4 may not only increase the amount of deposited Aβ but also increases microglia reactivity at the Aβ plaques (Rodriguez, Tai et al. 2014). This would also supports Amyloid hypothesis of AD through the indication of a gene present in such a large number of AD patients having an effect upon the accumulation of amyloid plaques. However, modern genome wide association studies (GWAS) have revealed a much larger number of genes that could have a potential effect on the pathology of AD, one study (Lambert, Ibrahim-Verbaas et al. 2013) revealed 19 potential susceptibility loci, 11 of which were newly discovered. A vast degree of the genetic risk of Alzheimer's remains unaccounted for; with more potentially involved genes being uncovered as the GWAS studies increase in power (see table 1). Worth noting is that APOE4 still remains the gene with the largest single effect, with the heterozygotic allele increasing susceptibility to AD by 3 times, and homozygotes for the allele having a risk 15 times greater than those without the allele (Blennow, de Leon et al.).

Gene name	Chromosomal location	Onset	Familial and/or sporadic	Involvement in AD
APP	**21q21.3–q22.05**	**Early**	**F**	**Certain**
PS1	**14q24.3**	**Early**	**F**	**Certain**
PS2	**1q31–q42**	**Early**	**F**	**Certain**
APOE	19q32.2	Late	S and F	Certain
α2M	12p	Late	S	Uncertain
LRP	12	Late	S	Uncertain
LBP-1c/CP2/LSF	12	Late	S	Uncertain
ACE	17q23	Late	S	Uncertain
VLDL-R	9pter–p23	Late	S	Uncertain
BChE	3q26.1–q26.2	Late	S	Uncertain
ACT	14q32.1	Late	S	Uncertain
IDE	10q23–q25	Late/early	S and F (?)	Uncertain
Tf C2	3q21	Late	S	Uncertain
catD	11p15.5	Late/early	S and F	Uncertain
BH	17q11.1–q11.2	Late/early	S	Uncertain
TGF-β1	19q13.1–q13.3	Late	S	Uncertain
5-HTT	17q11.1–q12	Late	S	Uncertain
APOE promoter	19q32.2	Late/early	S	Uncertain
NOS3	7q35	Late	S	Uncertain
CST3	20p11.2	Late	S	Uncertain
PS1 promoter	14q24	Early	S and F	Uncertain

Table 1 AD genetic factors
Genes involved in early-onset familial Alzheimer disease (bold) and susceptibility genes for AD

(Rocchi, Pellegrini et al. 2003)

1.2.5 Differences in onset rate according to gender

Current literature suggests that females are more prone to cognitive decline via AD than males (Rocca, Mielke et al.) (Li and Singh 2014). One possible explanation of this is that it may be due to the Aβ degrading enzyme neprilysin. Neprilysin has been implicated in many studies (Yasojima, Akiyama et al. 2001) (Iwata, Tsubuki et al. 2001) to be at high concentration in brain regions such as the hippocampus and cortex, both of which are areas associated with AD. The studies go on to determine that reduced levels of neprilysin in mouse models results in the dysfunctional regulation of Aβ and thus the models are more prone to AD pathology. Interestingly it may be this enzyme that accounts for the differences in disease onset rate between genders. In 3xTg-AD mice neprilysin levels decreased in both genders with age, but the rate at which the levels of this enzyme decreased are not consistent between genders (Hirata-Fukae, Li et al. 2008). 9 month-old male mice were used as a comparative point and assigned as the 100% point. At 9 months females were found to have only 87% of the amount of neprilysin when compared to the males, at 16 months both groups had a notable decrease, with males having 68% and females 58% compared to the 9 month male value. Though there is a slightly lower amount consistently in the female mice, this difference was not considered statistically significant, however at 23 months the difference was determined to have a statistical significance with 47% and 12% in males and females respectively. These findings may also translate well into a human model, with studies showing that neprilysin is up-regulated by oestrogen (Xiao, Sun et al. 2009) (Liang, Yang et al. 2010) and thus following the decline in oestrogen production following menopause levels of neprilysin in females would also decline, leading to an impaired ability to degrade Aβ. The study by (Hirata-Fukae, Li et al. 2008) also revealed that in the 3xTg-AD mouse model there is a higher level of beta-secretase in female mice, with the most pronounced difference between males and females occuring at 9 months, this difference was reduced at both 16 and 23 months, with females still having a slightly higher amount, but not by a statistically significant degree. Beta-secretase is partially responsible for the generation of the pathological Aβ-42, with beta-secretase deficient models having reduced amyloid deposition (Luo, Bolon et al. 2001), with this in mind a combination of increased beta secretase activity, potentially increasing amyloid load compared to males, with reduced amyloid degredation during later life, due to the reduction in levels of neprilysin may account for the higher number of Alzheimer's disease cases in females. This difference in disease occurance between the sexes, as well as the distinct increase in cases of AD with age was

illustrated in a study by (Gatz, Reynolds et al. 2006), with the findings shown in Figure four.

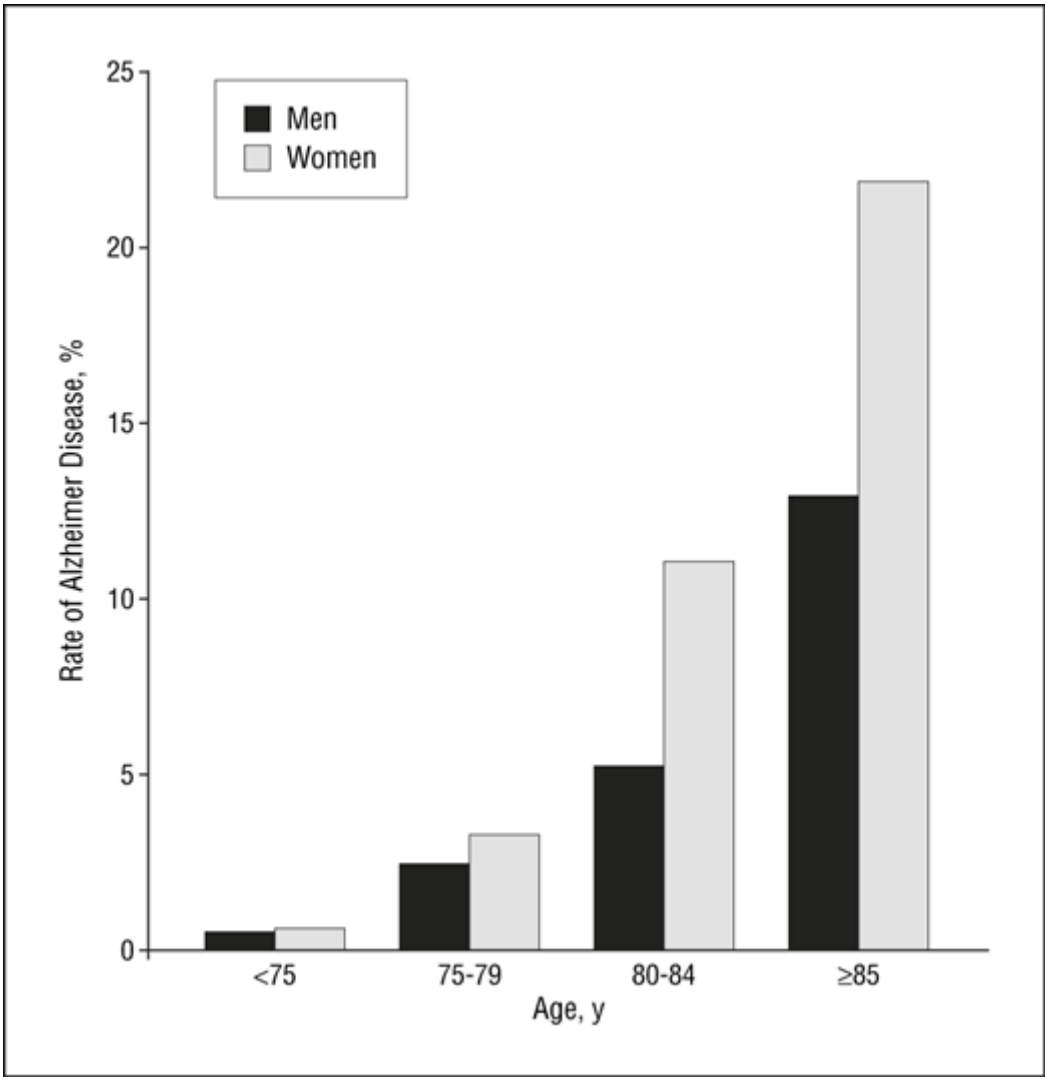


Figure 4 AD gender difference
Prevalence of AD by age group and sex.

(Gatz, Reynolds et al. 2006)

1.3 Model organisms of Alzheimer's disease

Historically several different models have been used for understanding the mechanisms of Alzheimer's disease, *Drosophila melanogaster* have previously been utilised as a model of AD, with discoveries including the effect of abnormal human tau protein causing death of neuronal cells akin to AD pathology (Williams, Tyrer et al. 2000). Zebrafish have also been utilised and many successes using this model have occurred due to the relative ease of manipulating genes (Newman, Nornes et al. 2012). Both model organisms suffer the drawback of a difficulty in studying behavioural changes, thus a more complex organism such as the mouse becomes a necessity in studying the cognitive effects of the disease. One of the most widely used approaches to AD research comes in the form of transgenic mice (LaFerla and Green 2012). These mice have been genetically engineered to produce a homozygous population containing, in the case of AD research, a human gene, or a number of human genes related to AD such as APP or Presenilin 1. Various mouse strains have been created (Bryan KJ *et al,* 2009) with the intention of analysing separate aspects of the disease, predominantly the mechanisms behind both Aβ pathology and tauopathy.

For the purposes of the study the APPswe/PS1ΔE9 model has been used, this transgenic strain expresses a chimeric human/mouse APP gene with Swedish mutations (K594N/M595L) as well as a mutated copy of the human presenilin 1 gene. The advantage of this combination of mutations being the aggressive rate of onset of amyloid plaque formation within the cortex and hippocampus, expressing plaques by age 5-6 months (Jankowsky, Fadale et al. 2004). By comparison expression of the APP mutation alone typically shows the formation of plaques after 24 months, thus with both mutations expressed the progression of disease pathology can be observed as the mice age and cognitive decline can be monitored. Levels of both Aβ-42 and Aβ-40 have been found to be increased in this strain of mouse, with a more significant amount of Aβ-42 present, which is implicated as the cause of the rapid formation of amyloid plaques. Interestingly this strain does not develop neurofibrillary tangles typical of AD pathology (Minkeviciene, Ihalainen et al. 2008), implying the role of mutated Tau proteins that are not present in the strain. Hippocampal neurochemistry is documented to be altered within APPswe mice, with impaired cholinergenic neurotransmission from 5-9 months (Goto, Niidome et al. 2008) as well as reduced levels of serotonin and noradrenaline at 18 months (Szapacs, Numis et al. 2004). Cognitive decline has been primarily tested via Morris water maze, with a deficit in memory and visuo-spacial learning beginning at 8

months (Minkeviciene, Ihalainen et al. 2008) with a progressive decline with age akin to that found in human AD pathology.

However one of the key issues faced is the translation from animal models to clinical trials involving humans (Geerts 2009). Suggestions as to the cause of this disconnection of animal models and human studies have included the differing targets of potential new drugs within the given model. Incomplete models are also an issue, with the disease pathology only partly understood; transgenic models are thus limited by only being able to incorporate a select few genetic alterations in each model, as such the complex interactions between both the vast number of genetic factors implicated as well as potential environmental stimuli leading to AD are never fully replicated. Further issues involve the homogenous nature of the model organisms, for example in the case of APP transgenic mice (Kokjohn and Roher 2009) the mutations causing the excess production and aggregation of Aβ are well documented, but are not representative of the entirety of Alzheimer's pathology. Transgenic models are limited by the fact that the mutated genes involved, including the APP gene, are representative of causes known to be involved in familial AD, which constitutes a small percentage of all AD cases (Blennow, de Leon et al.). In contrast, the overwhelming majority (Duara, Lopez-Alberola et al. 1993) of AD cases are sporadic (SAD) which is thought to occur through a combination of both genetics and environment, with the main risk factor being age. Such is the case that it is difficult to study the effects and mechanism behind sporadic Alzheimer's, but through combined use of many transgenic strains, singular aspects of the system may be analysed and applied to the whole.

1.4 Huntington's disease

1.4.1 Disease background

Huntington's disease is an autosomal dominant disorder characterised by an expansion in the repeated CAG (cytosine, adenine, guanine) triplet, coding for the amino acid glutamine (Q), located in the coding region *IT15* (interesting transcript 15) gene (Albin and Tagle 1995). The poly-glutamine (polyQ) region is responsible for the functional and pathological differences between the HTT (Huntingtin) protein and the mutant mHtt protein. The pathology and age of onset of the disease correlates to the length of the polyQ region (Langbehn, Brinkman et al. 2004), with 9 to 35 repeats constituting a normally functional HTT protein. With a repeat length of 36 to 39 the disease shows incomplete penetrance, symptoms may or may not be apparent, and typically in the case that symptoms are present the age of onset is comparatively high to those with 40 or more repeats. Due to the late onset coupled with a slow progression of disease pathology in some cases symptoms may never be noticed (Walker). In HD patients with an excess of 40 CAG repeats the disease is fully penetrant, with several studies documenting a negative correlation between the number of repeats and age of onset (Andrew, Paul Goldberg et al. 1993) (Snell, MacMillan et al. 1993). In patients with a high number of CAG repeats, typically above 60, onset of symptoms may occur as early as the age of 20 (Nance and Myers 2001), termed "juvenile HD" and constituting around 7% of the total number of HD patients. Juvenile HD is typically paternally inherited, with numerous studies documenting that the paternal allele is far more prone to extension of the CAG repeat with cases of 5 or more added repeats only observed from paternal inheritance (Nørremølle, Sørensen et al. 1995), thus a seemingly healthy individual may pass on an HD allele following a CAG expansion should the number of repeats increase above the threshold of 35.

1.4.2 Symptoms

Huntington's disease pathology is characterised by a triad of symptoms, involving motor, cognitive and psychiatric dysfunction. Studies have suggested that a number of subtle psychological differences occur in those positive for extended CAG repeats even before HD diagnosis (Duff, Paulsen et al. 2007), with the example study estimating the subjects to be more than 10 years prior to a clinical diagnosis already appearing more prone to symptoms such as depression, anxiety and obsessive-compulsiveness. By the time of diagnosis symptoms include dysfunction in motor systems (de Boo, Tibben et al. 1997) such as loss of muscular control leading to uncontrolled movements termed "chorea". Progressing over the course of HD pathology to the point that rigidity, difficulty walking, facial distortion and difficulty speaking become common, these symptoms have been shown to correlate with striatal atrophy occurring at the early stages of the disease (Montoya, Price et al. 2006). Weight loss has been attributed as a symptom of the disease (Aziz, van der Marck et al. 2008) through a combination of muscular issues leading to difficulty in both chewing and swallowing, as well as an increasing reliance as symptoms progress on assistance from carers. Cognitive decline is characteristic of the disease and well documented in both model organisms and human HD patients. In the early stages of the disease cognitive processes such as abstract thinking and planning are affected, as the disease symptoms progress a decline in memory is often observed (Stack, Kubilus et al. 2005). Psychiatric issues can also occur across the course of the disease, with symptoms ranging from paranoia to hallucinations as well as intellectual decline (Kirkwood, Su et al. 2001), often to the point that the patient requires institutionalisation for further care to be provided.

1.4.3 Aggregates of mutant huntingtin

The pathological hallmark of Huntington's disease is the formation of aggregates of cleaved products of mHtt (Schilling, Becher et al. 1999), interestingly the proposed pathogenic intranuclear inclusions (NII) are only detectable by Huntingtin antibodies specific to the N terminal of the protein (Sisodia 1998). This would indicate that after proteolysis a cleaved fragment at the N terminal, containing the polyglutamine (CAG) repeat sequence is capable of diffusing into the nucleus. It has long been thought that these nuclear inclusions are responsible for the pathogenicity of mHtt(DiFiglia, Sapp et al. 1997). However in studies following this evidence was found suggesting the opposite may be true, and that these inclusion bodies are a cellular coping mechanism designed to reduce the amount of the more toxic, soluble mHtt within the cell. The role of the NII is at this point highly controversial, with some studies indicating a toxic role, while others show no correlation between the rate of cellular apoptosis and the formation of inclusion bodies, other sources even suggest a protective effect. In a study by (Saudou, Finkbeiner et al. 1998) it was stated that mHtt in these nuclear inclusions were ubiquitinated in both human and mouse models of the disease, and that this was not the case for the healthy Htt protein, with these findings also confirmed in *in vitro* models. The study also showed that inhibition of ubiquitination of mHtt does inhibit the formation of NII, thus ubiquitination is a possible prerequisite of inclusion body formation. Further data from the study indicated that after the inhibition of inclusion body formation the rate of Huntingtin induced cell death was increased, supporting the claim that the NIIs are not the cause of pathogenicity. It has been suggested by other studies that rather than aggregated cytoplasmic or nuclear mHtt it is the soluble form of mHtt that is the cause of disease pathology (Arrasate, Mitra et al. 2004). The findings of this study indicated that neuron survival was more closely linked with mHtt dose and polyglutamine expansion length, with neurons also dying without forming a NII. Contrary to previous claims, the study found that formation of inclusion bodies within the nucleus lowered levels of mHtt elsewhere in the neuron, and increased neuronal survival, this supports the claim that the inclusion bodies are a means for the cell to reduce the amount of soluble mHtt. Other sources claim that the nuclear inclusions are indeed pathogenic, more so than cytoplasmic aggregates (Iwata, Christianson et al. 2005) since the cell is capable of removing the cytoplasmic aggregates via autophagy, while the nucleus provides a "safe haven" for the inclusion bodies, which are unable to be removed through the same process. There is also evidence of the nuclear inclusion bodies disrupting transcription (Nucifora, Sasaki et al. 2001), the study found that the transcriptional coactivator CREB

binding protein (CBP) was depleted in its regular location within the nucleus, and found within the nuclear aggregate of mHtt. It was proposed that mHtt due to its extended polyglutamine repeats allows for abnormal interactions with proteins containing short polyglutamine sequences. The abnormal localisation of CBP was found in HD cellular models and HD transgenic mice as well as the post mortem brains of human HD patients. To date the role of NII are still debated, with studies giving evidence for both pathogenic and protective effects.

1.4.4 Disease mechanism

The Htt protein interacts with over 100 different proteins (Goehler, Lalowski et al.), thus its function and the mechanism by which it induces cell death is currently poorly understood, it is however well documented that HD pathology predominantly affects the striatum, with evidence implicating the protein Rhes (Subramaniam, Sixt et al. 2009). This protein is specific to the striatum and has been found to induce sumoylation of mHtt, this may account for HD pathology's predominance within the striatum. The study established that within an HEK293T model, cell survivability was significantly reduced when co-expressing both Rhes and mHtt, indicating a potential cause of mHtt toxicity. The basal ganglia is documented to be among the first regions effected by HD pathology (Browne, Bowling et al. 1997), with suggestions that increased levels, or alternatively increased sensitivity to glutamate leading to excitotoxicity and eventually cell death (McGeer and McGeer 1976). Alternative mechanisms have been proposed involving the effect of mHtt on mitochondria, either through a direct interaction or indirectly via mHtt's effects on gene transcription (Browne 2008) leading to dysfunctional regulation of metabolism in affected neurons, potentially causing cell death. Mutant huntingtin has also been shown to disrupt axonal transport due to mHtt aggregation (Shirendeb, Calkins et al. 2012) (Lee, Yoshihara et al. 2004), potentially leading to the abnormal build-up of proteins (Vos, Grierson et al. 2008), which as shown (Di Stefano, Nascimento-Ferreira et al. 2015) can signal for apoptosis to occur.

Currently there is no known cure for Huntington's disease, though medication is available to manage some of the symptoms such as tetrabenazine, a drug designed for treatment of hyperkinetic movement disorder for the management of chorea (Frank and Jankovic 2010). Other strategies include the use of anti-psychotics for the management of delusions and hallucinations, as well as anti-depressants in the case of depressive symptoms (Bonelli, Wenning et al. 2004).

1.5 Models of Huntington's disease

Various species are currently in use as model organisms for Huntington's disease, simple cellular models such as HEK293T (Subramaniam, Sixt et al. 2009) and HeLa cells (Wyttenbach, Carmichael et al. 2000), have previously been used for protein expression or co-localisation studies. Invertebrates such as *Drosophila* have also been utilised, with studies providing information regarding axonal degeneration and transport (Lee, Yoshihara et al. 2004). Vertebrate models have the advantage of being more closely related to humans, as well as providing a useful model for behavioural studies, with a large number of advancements taking place in mouse models (Menalled 2005). As HD has been determined to be caused by a single gene mutation, this has become a focus of study, with knock-in, knock-out and transgenic mice strains created for this purpose. Knock in strains are commonly utilised as a genetic mimic of the human HD gene (Deng, Wong et al. 2014), with various strains containing differing poly-glutamine repeat lengths.

This study has used two model organisms for both *in vivo* and *in vitro* studies of the mechanisms of Huntington's disease. Firstly, the Q140 knock-in strain of mice, a well characterised (Menalled 2005) and widely used strain, showing a relatively slow onset of disease pathology with aggregates of mHtt present at around 4 months with the behavioural phenotype stated as hyperactivity beginning at 1 month, followed by hypoactivity from 4 months onwards, a gait deficit is noted as of 24 months. This was further demonstrated in a study by our own lab (Marangoni, Adalbert et al. 2014) illustrating the progression of the disease between the ages of 4 and 12 months and showing the progressive formation of nuclear inclusions in the striatum. The Q140 strain was selected for this study as the intention was to study neuronal pathology at the early stages of the disease. At the 6 month time point Q140 mice are shown to have NIIs (Marangoni, Adalbert et al. 2014) without demonstrating any sign of striatal neuron loss (Rising, Xu et al. 2011), providing a model comparable to pre-symptomatic HD in humans.

Alongside the in vivo work in mouse models of Huntington's disease an in vitro model using Human embryonic kidney (HEK 293) cells was utilised to study the possible interactions between Htt and NMNAT2. HEK293T cells have previously been used successfully in the study of HD pathology, being utilised in the study of the interaction between mHtt and Rhes.

The HEK293T model has been widely used previously as a means to study protein-protein interactions (Lim, Hao et al. 2006), utilising the HEK293T cells in conjunction with DNA from, for example a plasmid vector, to express exogenous proteins for use in in vitro

experimentation. This model benefits from fast growth time and ease of which protein interaction can be studied, for instance the interaction between mHtt and Rhes was demonstrated in the study by (Subramaniam, Sixt et al. 2009), in which proteins were transfected individually as well as being co-transfected, with cells expressing both proteins showing a significantly reduced survival rate.

1.6 Memantine and FK866/NA

1.6.1 Memantine

Memantine is currently utilised in the treatment of moderate to severe cases of AD (Mount and Downton 2006) under market names such as Memox and Namenda. It has been determined by various studies that one of the key mechanisms of memantine in regards to its action against AD and dementia is its function as a non-competitive N-methyl-D-aspartate (NMDA) receptor antagonist (Johnson and Kotermanski 2006) (Danysz and Parsons 2012). It is the fact that memantine is an uncompetitive inhibitor that allows it to function as an NMDAR antagonist without disturbing normal neuronal function, it is capable of binding the receptors at a greater affinity then Mg^{+} ions though does not have a such a high affinity that it interferes with synaptic signalling (Xia, Chen et al. 2010). This allows for the limitation of excitotoxicity caused by a continued influx of calcium ions from sources such as extra-synaptic signalling. Memantine does appear to show some degree of selectivity, targeting extra-synaptic "death" receptors more favourably than synaptic receptors (Xia, Chen et al. 2010), again allowing regulation of Ca^{+} influx without preventing signalling.

Despite both *in vivo* and *in vitro* studies primarily focusing on the role of memantine as an antagonist to NMDA receptors, other novel mechanisms of memantine have been proposed. A study by Wu *et al*(Wu, Tzeng et al. 2009) has proposed two different examples involving microglia and astroglia, suggesting that the neuroprotective effects of memantine are at least partly due to a stimulation of release of neurotrophins by astroglia, as well as anti-inflammatory properties via the inhibition of microglia activation. Other studies have also confirmed that treatment with memantine inhibits the activation of microglia (Takeda, Muramatsu et al. 2009), in the context of an AD model this anti-inflammatory effect could potentially play a key role. However some studies show that though memantine confers a protective effect, there is little evidence of any cognitive improvement, particularly in the early stages of AD (Schneider, Dagerman et al. 2011), by the mid to late stages of AD development several studies show that memantine seems to show a more pronounced positive effect (Gauthier, Loft et al. 2008) (Reisberg, Doody et al. 2003) though due to the nature of neurodegeneration drastic improvements are not expected, rather memantine shows itself to be useful in terms of delaying the rate of disease pathology.

1.6.2 FK866

Currently there are very few studies of the functions of FK866, with its only investigated role being its ability to inhibit the enzyme Nicotinamide phosphorybosyltranferase (NAMPT) (Hasmann and Schemainda 2003) (Pittelli, Formentini et al. 2010), responsible for the formation of the intermediate molecule nicotinamide mononucleotide (NMN) during the nicotinamide adenine dinucleotide (NAD) synthesis pathway. Due to the ability of FK866 to manipulate the production of NAD it has been used in the study by Hasmann and Schemainda as a means of promoting cellular apoptosis in diseases in which regular cellular apoptosis has become dysfunctional, for example in the instance of tumours. By depleting NAD reserves through inhibition of the formation of NMN, FK866 is capable of inducing apoptosis, as such it was implicated as having potential use in the treatment of cancer, though suffers the drawback of its lack of specificity, thus if applied in an *in vivo* model the same NAD depletion based apoptosis would occur in healthy cells as well as tumour cells. The study by (Di Stefano, Nascimento-Ferreira et al. 2015) has shown that NAD can be provided via a separate pathway by the addition of Nicotinic acid (NA), thus allowing for the effect of FK866 in inhibiting the rise in NMN, while still providing the cell with a pathway to produce NAD and so preventing cell death from NAD depletion.

1.7 Aims and objectives

The effects of memantine are already well documented in the literature, and studies have already shown the protective effect against the progression of Huntington's disease (Beister, Kraus et al. 2004), the effects of FK866 in the context of a disease model are yet to be established. With axonal transport deficits in both AD and HD potentially mimicking the accumulation of NMN as shown by (Di Stefano, Nascimento-Ferreira et al. 2015) the focus of this study is the investigation of the effects of FK866/NA within the Q140 knock-in HD model mouse, as well as the APPswe/PS1ΔE9 transgenic AD model. Secondary to this, following prior results by the lab showing a co-localisation of NMNAT2 and Htt the investigation of a potential interaction between the two proteins will be conducted via *in vitro* experiments using the HEK293T model in order to establish whether Htt plays a role in the axonal transport of NMNAT2.

2 Materials and methods

2.1 Mouse origins, breeding and treatment prior to tissue collection

Homozygous HdhQ140 ($Hdh^{Q140/Q140}$) (Menalled, Sison et al. 2003) and APP_{swe}/PS1dE9 (Jankowsky, Slunt et al. 2001) alongside the non-transgenic littermates were crossed with Thy1.2-YFP-H homozygotes on a C57BL/6 background (Berman, Westbrook et al. 2000) in order to produce heterozygous HdhQ140/YFP-H ($Hdh^{Q140/YFP-H}$) and APP_{swe}/PS1dE9/YFP-H mice, expressing the yellow fluorescent marker protein (YFP) in a subset of neurons. All mice were obtained from The Jackson's laboratories (USA) and were kept at The Bio Support Unit at The University of Nottingham. All breeding and procedures were performed as authorized under The Animals Scientific Procedures Act 1986 under project licence 40/3601.

Mice had been divided into three treatment groups for the purpose of the study at the age of 5 months and 2 weeks:

- Vehicle treated (injected with vehicle, no medication administered)
- Memantine (20mg/kg/day administered via injection)
- FK866/Nicotinic acid (FK866 injected at 15mg/kg/day, Nicotinic acid co-administered orally via drinking water at 50mg/kg/day)

Mice had been subject to the following behavioural testing following drug administration:

- Sensorimotor: rotarod, open field, prepulse inhibition.
- Learning, memory and anxiety: Elevated plus maze, spontaneous alternation.

Finally the mice had been culled and perfused, the brains were then collected for use in this study. Numbers are as follows:

Mouse group/gender	Number of males	Number of females
APP_{swe}/PS1dE9 Memantine	4	4
APP_{swe}/PS1dE9 FK866/NA	4	4
APP_{swe}/PS1dE9 vehicle	4	4
Q140 Memantine	3	3
Q140 FK866/NA	3	3
Q140 vehicle	3	3

2.2 Cryostat sectioning

Brain samples were removed from storage at -80°C shortly before sectioning and kept at -20°C inside the Leica 3050 cryostat for roughly 15 minutes. The half brain was mounted in preparation for sagittal sections using OCT to mount to the chuck and to encase the brain. Sections were cut to a 20µm thickness and transferred directly to 24 well containers to rehydrate for roughly 45 minutes before mounting to Superfrost slides.

2.3 H&E staining

A single brain section was mounted directly to a slide and submerged in running tap water for 30 seconds, followed by a 5 minute incubation in Harris Haematoxylin. The slide was then washed in tap water until the section cleared, proceeded by dipping in acid alcohol for 5-10 seconds. Slides were then washed in tap water until there were no longer any streaks, then dipped in lithium carbonate/Scott's tap water for 1 minute and washed in running tap water for a few seconds. Samples were checked for a blue stain via microscope before being submerged in 1% Eosin for 5 minutes. Slides were washed again in running tap water for a few seconds before being dipped in 50%, 70%, 90% and 100% alcohols respectively (2 seconds each). Finally the samples were dipped in fresh Xylene for 2 minutes, again in finishing xylene before adding a few drops of DPX and placing on the coverslip.

2.4 Immunohistochemistry

Before commencing the immunohistochemistry protocols a number of brain sections were first treated with an antigen retrieval protocol using sodium citrate solution (2.35g sodium citrate, 800ml dH2O, pH6.0, 0.05% Tween-20) with the hopes of exposing more antigen sites for more efficient antibody penetration. Brain sections previously mounted to Superfrost slides and air dried were then submerged in the solution and incubated overnight at 55°C, the following day these slides were then removed from the solution and briefly washed for 10 minutes with PBS. Following this the immunohistochemistry procedures were followed as per protocol

Following sectioning via cryostat the brain sections were rehydrated in PBS for around 45 minutes then mounted to superfrost slides and allowed to air dry, the slides were then either put through the antigen retrieval protocol or directly stained. Firstly the mounted brain sections were blocked using a solution of PBS containing 5% goat serum for 1 hour. The blocking buffer was then removed and the primary antibody (in PBS with 5% goat serum) was added (see table at end of protocol) and allowed to incubate overnight at 4°C. The following day the primary antibody was removed and the slides washed in PBS on a rocker at RT for 15 minutes three times. The secondary antibody was then added, again in a solution of PBS with 5% goat serum (consult table for antibodies) and incubated for 1 hour at RT. The secondary antibody was removed and a further three washes with PBS at RT for 15 minutes were performed before allowing the slides to air dry for 10 minutes before the addition of Vectashield and the cover slip. For the Q140 mice following the 3 washes after the secondary antibody a 10 minute incubation with 1:500 Hoechst stain (in 1% Triton X-100, 1x PBS) was used to stain the nuclei, this was followed by three brief five minute washes before air drying and adding the coverslip.

Primary antibody	**Secondary antibody**
α-Amyloid beta (1:2000)	Alexa fluor 568 α-mouse (1:200)
α-Huntingtin (1:1000)	Alexa fluor 568 α-mouse (1:200)
α-Microglia (1:2000)	Alexa fluor 405 α-rabbit (1:200)

2.5 Image acquisition

All images for both APPswe and Q140 mice were acquired via a Zeiss 710 confocal microscope using the Zen programme. For the amyloid plaque quantification single plane images were taken using a 10x air objective across the entirety of the cortex. In the case of the Q140 mice in order to quantify the nuclear aggregates of Huntingtin a 63x oil objective was used and three images were taken both in the striatum dorsal and striatum ventral (See figure five), z-stack images were acquired across a 10μm depth at 1μm intervals.

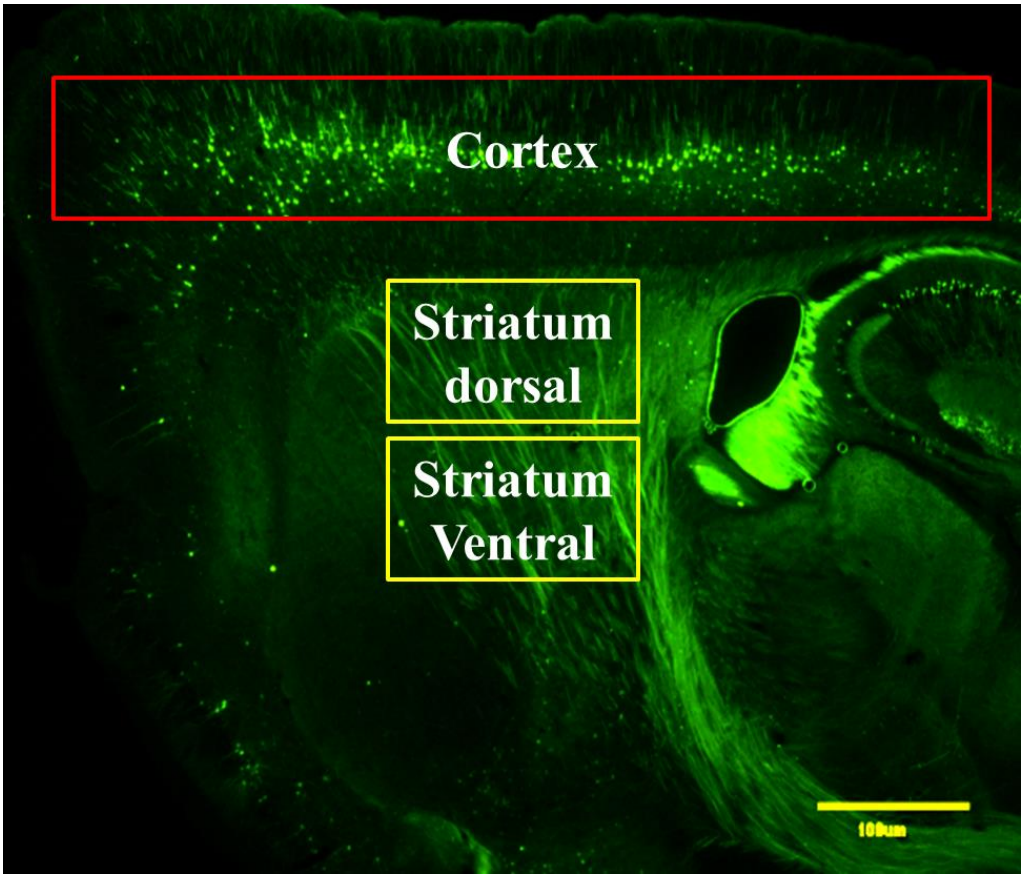


Figure 5 Brain analysis regions
Brain regions analysed across the study, with the cortex imaged in AD model mice for the purpose of quantifying amyloid plaques, and the two striatal regions analysed in HD model mice to quantify nuclear aggregates of mHtt.

2.6 Data acquisition and analysis

Following image acquisition via confocal microscopy the APPswe images were analysed manually using ImageJ, using the program to assess both the number of plaques as well as calculating the size of the plaques. Z-stack images acquired from the Q140 mice were analysed using the Zen program, 3D reconstructed images were analysed to quantify and assess location of nuclear aggregates of mHtt. In both cases the data was inserted into the Graphpad Prism program and statistical tests (multiple t-test with Welch's correction) were performed, these data were then used to create graphs containing both the standard error of mean (SEM) and an indication of statistical significance.

2.7 HEK293T cell cultures

Human embryonic kidney (HEK) cells were thawed at 37°C and plated into a 75T flask containing 15ml of Dulbecco's modified eagle medium (DMEM) (+1% L-Glu, 1% P/S, 10% FCS), these cells were then allowed to grow in an incubator at 37°C with 5% CO_2. HEK cells were passaged once every 4 days unless removed for usage. The medium was removed and the flask washed with 5ml of PBS. 3ml of trypsin (0.25%) was added to detach the cells from the flask; the flask was shaken then incubated at 37°C for 5 minutes. After further shaking the flask was checked under a standard bright field microscope to ensure the cells had detached, then 7ml of DMEM was added to inactivate the trypsin. The cell suspension was then transferred to a falcon tube and centrifuged at 1200g for 5 minutes. The supernatant was removed, the pellet was re-suspended in 5ml of DMEM and 1ml of the cell suspension was transferred to a new flask. Cells were grown in 15ml of DMEM at 37°C with 5% CO_2.

2.8 Transfection of HEK cells

One day before transfection, $3x10^6$ HEK293T cells/ml were plated in each of three separate petri dishes (~10cm diameter) containing 10ml of DMEM (+1% L-Glu, 1% P/S, 10% FCS) to allow cells to reach ~80% confluence before transfection. On the day of the transfection the DMEM in each dish was removed and replaced with 7ml Opti-MEM reduced serum medium (Thermo Fisher Scientific). For each plate a 24µg of HTTQ23 plasmid DNA (see appendix) was added to 1.5ml of Opti-MEM, the following was prepared for the three plates:

HTTQ23-His-mCherry 586 1λ (8.02 ug/ul)	**HTTQ23-His-mCherry 586 1λ (8.02 ug/ul)**	**No DNA (NC)**
3.0ul (24ug)	3.0ul (24ug)	-

Alongside this 60µl of Lipofectamine 2000 was added to 1.5ml of Opti-MEM, mixed and incubated at RT for 5 minutes. The lipofectamine and DNA samples were mixed (total volume 3ml) and incubated at RT for 20 minutes. These solutions were then added drop by drop to their allocated HEK cell plate and mixed by gently. Cells were incubated at 37°C in a CO_2 incubator for 6 hours, after which the medium was replaced with DMEM (+1% L-Glu, 1% P/S, 10% FCS). After 2 days the cells were viewed under a standard fluorescent microscope to check for mCherry expression.

2.9 Preparation of HEK cell whole cell extract

Lysis buffer was prepared prior to starting (20mM HEPES pH7.5, 250mM NaCl, 0.5% IGEPAL with a protease inhibitor added last as its effective time is ~1 hour). The plates containing the HEK cells were kept on ice. The growth medium was removed, the plates then rinsed twice with PBS and the cells scraped in 500µl of PBS and transferred to Eppendorf tubes. The cell suspension was centrifuged at 300g for 5 minutes then the supernatant was discarded. Cells were resuspended in 500µl of the lysis buffer and kept on ice for 20 minutes with occasional vortexing to facilitate efficient lysis. Following the incubation the cell suspension was centrifuged at 12,000xg for 10 minutes at 4°C. Aliquots of the supernatant from each sample were taken (20µl diluted with 5µl laemmli buffer for SDS-PAGE). The remaining supernatant was transferred to the beads according to the following plan:

500ul whole cell extract (WCE) with HTT Q23	500ul WCE with HTT Q23	500ul plain WCE (negative control NC)
NMNAT2-GST	GST (NC)	NMNAT2-GST

2.10 Transformation of *E.Coli* with p-GEX-NMNAT2

High salt versions of LB broth and LB agar were prepared and autoclaved, ampicillin (50µg/ml) was added to the agar solution once it had suitably cooled and then several agar plates were produced. An aliquot of competent DH5α cells were thawed on ice and aliquots were transferred to Eppendorf tubes. 1µl of the p-GEX-NMNAT2 plasmid (see appendix) was added and incubated on ice for 30 minutes. Cells were then heat shocked at 42°C for 50 seconds before a further 2 minute incubation on ice. 1ml of the sterile LB media was added to the cells and incubated at 37°C for a further 1 hour. The cells were then centrifuged at 1000rpm for one minute and 700µl of the supernatant was discarded. The remaining 300µl of cell suspension was plated in LB agar plus ampicillin (50µg/ml). The cells were then allowed to grow overnight at 37°C. The following day single colonies were picked, re-suspended in 3ml of LB agar plus ampicillin (50µg/ml) and incubated overnight in a rotating incubator at 37°C and 200rpm.

2.11 Protein expression

1.5ml of the overnight culture obtained from the (2.12 Transformation of E.Coli with p-GEX-NMNAT2) protocol was inoculated into 150ml of pre-warmed LB media + ampicillin and left to grow on a rotary incubator at 37°C and 225rpm. When the optical density (OD_{600}) of the suspension was ~0.5 a 20µl sample was taken, mixed with 5µl of 5x Laemmli sample buffer, boiled at 100°C for 5 minutes and microcentrifuged at 5000rpm for 1 minute .The sample was labelled as "BI" (before induction) and stored at -20°C before use. 0.5mM isopropyl-beta-D-thiogalactopyranoside (IPTG) was added to the flask and the cells were placed back in the rotary incubator at 30°C for 3 hours. Another 20µl aliquot was collected as above. The sample was labelled as "AI" (after induction) and stored at -20°C before use. Bacterial suspensions were spun at 4000g for 10 minutes in a pre-cooled centrifuge at 4°C. The supernatant was discarded and the resultant pellet was frozen at -20°C until needed.

On the day of use the pellet was thawed on ice and resuspended in 6ml of PBS (pH7.3) containing a protease inhibitor cocktail (Roche complete mini, EDTA free) and DNase I (25µg/ml) with MgClg/ml) with $MgCl_2$ (10mM). Cells were placed on ice and broken via sonication, over a period of 10 minutes per sample. The cell lysate was then centrifuged at maximum speed (~17,000rpm) at 4°C for 30 minutes, the supernatant was then removed, placed in a fresh tube and the centrifugation was then repeated. A 20µl sample of the supernatant was taken and added to 5µl of 5x Laemmli buffer, boiled for 5 minutes, centrifuged to spin down the condensation, labelled as Sup (supernatant) and frozen for SDS-PAGE. The remaining supernatant was then bound to Glutathione Sepharose beads.

2.12 Pull down assay

Binding of GST to beads

Beads preparation
150µl of re-sespended Glutathione Sepharose beads (75% slurry) was transferred into a 15ml falcon tube. The solution was then centrifuged at 500g for 5 minutes at 4°C, the supernatant was discarded. 1.5ml of chilled dH_2O (10x the volume of beads) was added and centrifuged using the same settings, followed by three more washes in PBS.

Binding
The cell lysate from (2.14 Protein extraction) was added to the beads and incubated at 4°C on a rotary wheel overnight. After the incubation the cells were spun at 500g for 5 minutes at 4°C and the supernatant removed after taking a 20µl sample for SDS-PAGE. The beads were then washed three times with 1.5ml of chilled PBS, each time being left for 15 minutes on a rotary wheel at 4°C and samples of the supernatant extracted for SDS-PAGE.

The HTTQ23 whole cell extract (WCE) was added to the beads and incubated on a rotary wheel for 3 hours at 4°C followed by a second incubation at room temperature for 30 minutes. From each sample a 20µl aliquot was taken as above and stored for SDS-PAGE. The remaining flow through was collected and frozen, the beads were then washed three times with 1.5ml of PBS, incubating each time for 15 minutes at 4°C on a rotary wheel and taking samples for SDS-PAGE after each wash. After the final wash the beads were resuspended in 200µl of fresh PBS, to this 50µl of 5x Laemmle sample buffer was added and the solution boiled at 100°C for 5 minutes. The condensation was microcentrifuged and frozen at -20°C ready for SDS-PAGE.

2.13 Co-immunoprecipitation of NMNAT2 and HTTQ23

HEK cells were transfected with the following plasmids:

- NMNAT2-Flag + HTT Q23
- Flag +HTT Q23
- NMNAT2-Flag

The cells were allowed to incubate at 37°C in a six well plate for 2 days, at 70-90% confluence growth medium was removed and the cells washed once with PBS kept on ice, PBS was removed and 700µl of lysis buffer (50 mM Tris HCl, pH 7.4 with 150 mM NaCl, 1 mM EDTA, and 1% TRITON X-100) was added alongside a protease inhibitor cocktail (Complete mini EDTA free). Cells were scraped and collected via pipette before being transferred to an Eppendorf tube. The cells were kept on ice for 30 minutes, during which they briefly placed on the vortex every 5 minutes to ensure maximum exposure to the lysis buffer and prevent sedimentation. Following the 30 minutes incubation the lysate was centrifuged for 10 minutes at 12000xg, the supernatant was then transferred to a fresh Eppendorf and kept on ice.

The ANTI-FLAG M2 affinity gel (Sigma-Aldrich, catalogue number: A2220) was thoroughly re-suspended within the vial, 40µl of which was transferred to a fresh tube (pipette tip cut in order to allow transfer of beads) and centrifuged for 30 seconds at 5000xg, allowing a few minutes afterwards for the beads to settle. The supernatant was removed using a narrow ended pipette tip and the resultant beads were washed twice with 0.8ml of TBS (50 mM Tris HCl, with 150 mM NaCl, pH 7.4). The TBS was removed after the washes and 700µl of the cell lysate was added to the resin (At this stage a separate sample of resin was combined with lysis buffer with no cell lysate as a negative control (NC)). All samples were incubated for 2 hours at 4°C on a rotator. After the incubation the samples were centrifuged at 5000xg for 30 seconds.

The supernatant was removed with a narrow ended tip and a sample of 20µl combined with 5µl of 2x SDS sample buffer (125 mM Tris HCl, pH 6.8, with 4% SDS, 20% (v/v) glycerol, and 0.004% bromphenol blue) and boiled at 100°C for 5 minutes before being frozen in preparation for SDS PAGE (Labelled as Flow through (FT)). The resin was washed a further 3 times with 0.5ml of TBS and each sample prepared for SDS PAGE as detailed above.

2.14 SDS-PAGE

22µl of each sample taken during the pull down assay were loaded to an SDS-PAGE gel and run at 120V for 20 minutes, to allow for proteins to pass through the stacking buffer, then at 200V for 40 minutes.

In the case that multiple gels had been run using copies of the same, one gel was stained with coomasie blue to check for overexpressed proteins before proceeding with the western blot.

2.15 Western blot

The acrylamide gel was removed from the glass plates and equilibrated in 1x transfer buffer (10% methanol 240mM tris, 1.95M glycine, 0.5% sodium dodecylsulphate) for 10 minutes. Proteins were transferred to a nitrocellulose membrane at 350mA for 1 hour and 30 minutes using a wet transfer.

The membranes were then washed with PBS-T (0.2% tween-20) for 1 hour at RT, followed by a 1 hour block at RT in PBS-T (0.2% tween-20) +5% milk. After this the membrane was incubated with the primary antibody:

-Monoclonal anti-polyHistidine (Sigma Aldrich, cat number 028k4856), diluted 1:3000 in PBS- T (0.2% tween-20) +5% milk, incubated 2 hours at 4°C and a further 1 hour at RT.

-Monoclonal anti-HTT (Fisher Scientific, cat number mab2166) diluted 1:1000 in PBS- T (0.2% tween-20) +5% milk incubated O/N at 4°C

-Monoclonal ANTI-FLAG M2 (Sigma Aldrich, cat number F7425) diluted 1:1000 in PBS- T (0.2% tween-20) +5% milk incubated O/N at 4°C

The membrane was then washed with PBS-T three times for 15 minutes each and then incubated with Anti-mouse IgG peroxidase (GE Healthcare, cat number Rpn4201V) (1:3000 diluted in PBS- T +5% milk) as the secondary antibody for 1 hour at RT. After a further three washes of 15 minutes in PBS-T were applied, the membrane was treated with a chemiluminescence detection kit for Horseradish peroxidase (HRP) (GE Healthcare, cat number Rpn2106) according to the manufacturer’s instructions and then placed in an x-ray cassette and exposed.

2.16 Preparation of Superior cervical ganglia dissociated cells

Mouse pups were culled by cervical dislocation and superior cervical ganglia were dissected and placed in a DMEM solution before being cleaned and transferred to a fresh dish.

25µl of Laminine (23017-015 Invitrogen) was diluted in 1.25ml DMEM (Sigma DMEM 6546), 50µl was added to the centre of each Ibidi dish and left for 1 hour. The cleaned ganglia were placed in a falcon tube containing 5ml of trypsin solution (Sigma T9201, 0.25mg/mL in PBS) and incubated at 37°C for 30 minutes. Collagenase type II solution was prepared in a 5ml Bijou tube filled with PBS by adding a small amount of the collagenase powder until the solution turned brown. The trypsin was removed from the ganglia and the collagenase solution was filtered into the falcon tube using a 0.22µm syringe and the resultant solution was incubated at 37°C for 20 minutes. Roughly 50µl of DMEM was prepared per Ibidi dish and kept at 37°C, shortly before adding to the ganglia a 1:1000 concentration of both Aphidicolin (4µm, Sigma) and nerve growth factor (NGF) (100ng/ml, Invitrogen) was added. The collagenase solution was removed and replaced by 1ml of the prepared DMEM medium, suspended cells were then pipetted up and down until the ganglia had broken and the solution was homogenous. The solution was centrifuged at 300xg for 5 minutes and the supernatant was removed. 50µl of the prepared DMEM was added to the pellet per Ibidi dish and after re-suspension 50µl of the resultant solution was added to the centre of each dish and allowed to incubate.

2.17 Microinjection of SCG cells

Following a period of 24 hours the Ibidi plates were taken out of incubation and placed in a Zeiss Axiovert S100 microscope equipped with an Eppendorf Femtojet transjector and a 5171 micromanipulator system. A solution of 1x PBS, dH_2O, along with the NMNAT2-GFP (0.1µg/µl) and Htt-mCherry (0.05µg/µl) plasmids was prepared and passed through a Spin X filter into a microinjection capillary tip (Eppendorf Femtotip, Fisher Scientific). Roughly 150 nuclei were injected per dish. These cells were then placed back in incubation at 37°C for 12-24 hours and then analysed via TIRF microscope.

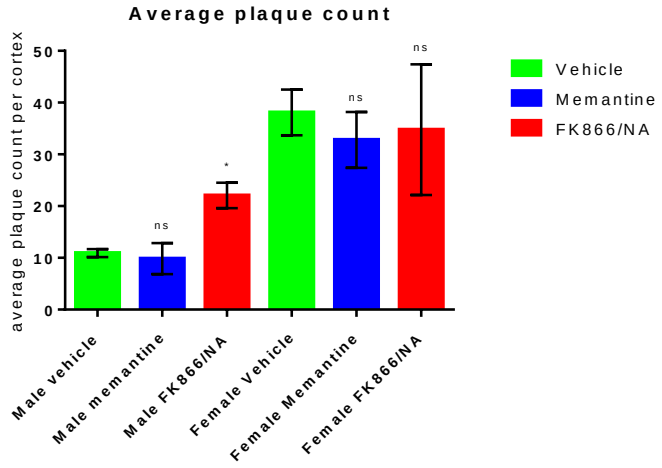
3 Results

3.1 Neither memantine or FK866/NA were found to significantly reduce plaque count in the APPswe/PS1ΔE9 mouse model

A previous study conducted within the lab (O.Othman, unpublished PhD 2015) revealed that axonal dystrophies, shown to co-localise with amyloid plaques, were found to be reduced following treatment with both memantine and FK866 in the cortex of APPswe/PS1ΔE9 mice. One of the aims of my study was to assess the effect of the medications on amyloid plaques and with this previous data in mind the hypothesis was that amyloid plaques would show a correlative decrease with the dystrophies. The images of the cortex were taken as detailed in the methods section, with an average taken of 5 cortex sections per mouse, with 4 mice analysed per gender/medication group.

In contrast to the original hypothesis it was found that no significant reduction in plaque number was found in either medication group (See figure six). Memantine treated mice showed little deviation from the vehicle treated control group, with no significant results. Surprisingly it was found that in the mice treated with FK866/NA the number of plaques showed a statistically significant rise within male mice ($P=0.0158$), the female group did not show a significant rise in plaques, however as demonstrated by the SEM bar on the graph in figure six there was a high variability within the group, with some having a higher number of plaques and some having fewer. Worth noting is that the larger number of dystrophies previously documented in the female mice compared to the males is consistent with my data, females were always found to have a higher plaque number than their male counterparts in all treatment groups.

A



B

Mouse group (compared to corresponding vehicle group)	P value (via unpaired t test)
Male memantine	0.7491
Male FK866/NA	0.0158
Female memantine	0.4774
Female FK866/NA	0.8161

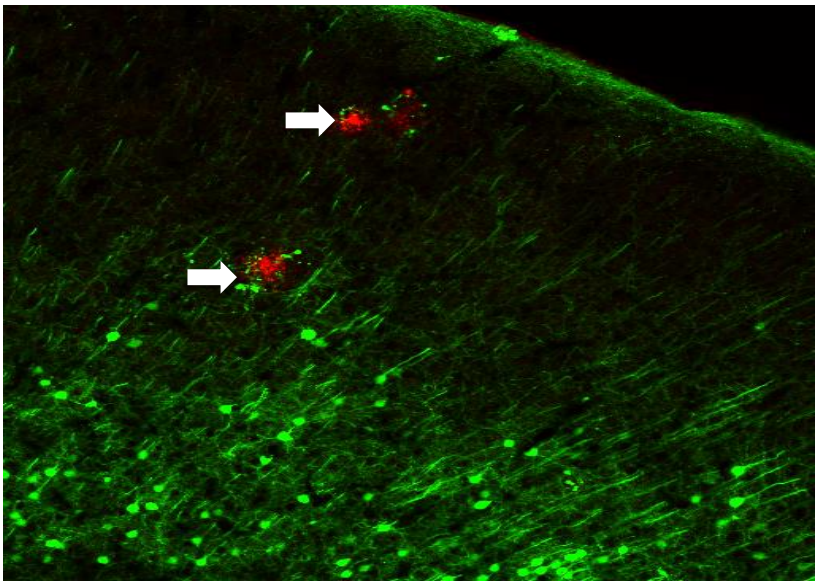
Figure 6 Average plaque count

(A) Images of sagittal brain sections were taken using confocal microscopy using a 10x air objective and quantified manually via Zen lite. Results of the quantification of plaques were expressed as the average plaque count per cortex, N=4 per gender/medication group with five sagittal sections quantified per mouse. Results displayed as mean +/- SEM, statistical analysis performed using unpaired t-test with Welch's correction. ns P>0.05, *P<0.05, **P<0.01, ***P<0.001, ****P<0.0001, compared with vehicle treated.

(B) P values corresponding to the graph

With regards to the co-localisation between plaques and dystrophies, it would seem the case that where a dystrophy is present, there is also a corresponding plaque (see Figure 7A). There were a small number of exceptions to this case, though these dystrophies had a faint red signal present, suggesting that it may be the case that there is still a localised plaque at a different plane. The opposite was true in the case of plaques, with numerous cases of plaques being present with no corresponding dystrophy (Figure 7B), this is consistent with the literature stating plaques as a prerequisite of the formation of dystrophies.

A



B

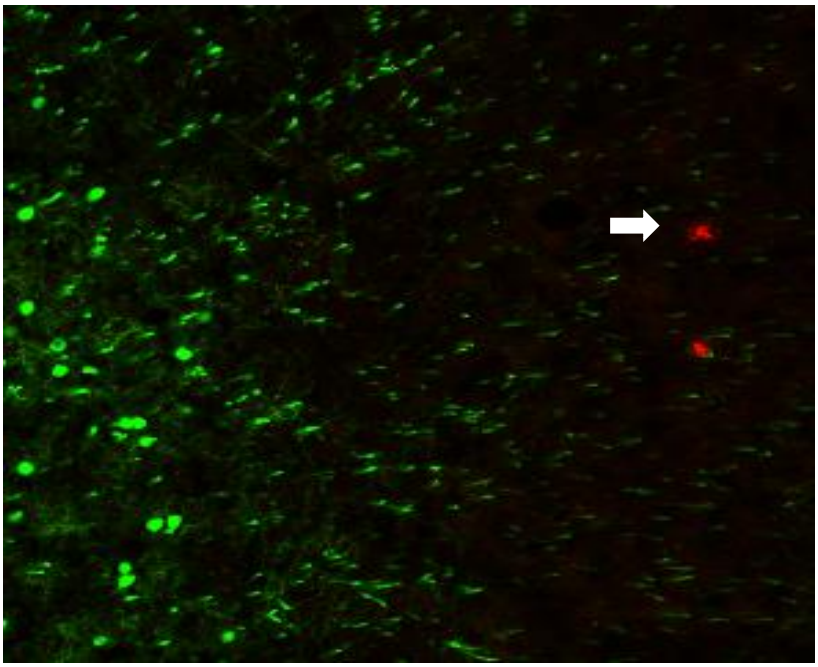
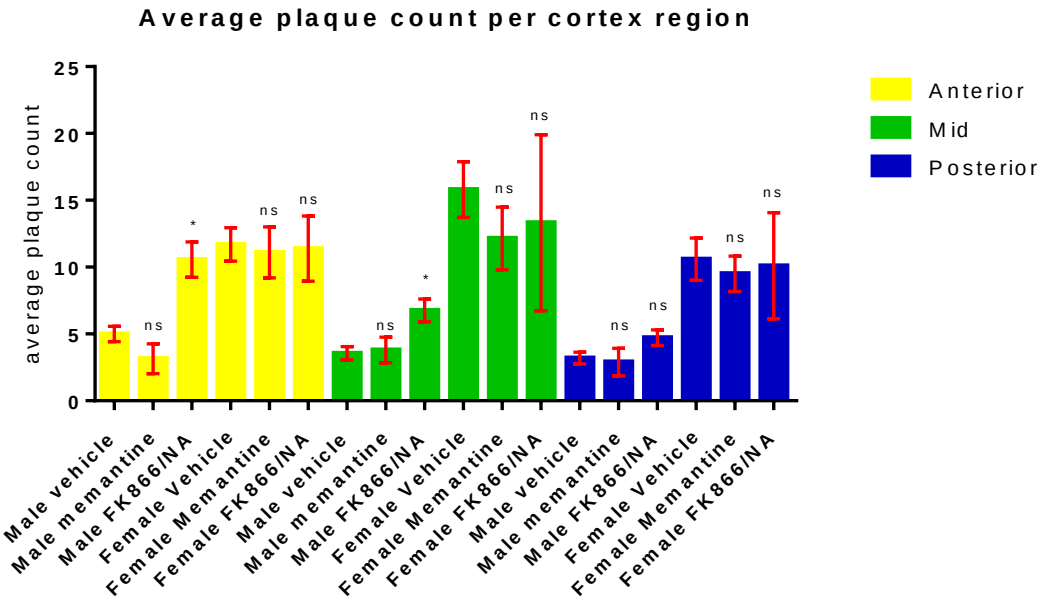


Figure 7. Plaque and dystrophy colocalisation
Images acquired via confocal microscopy using a 10x air objective, APPswe/PS1ΔE9 mice crossed with Thy1.2-YFP-H homozygotes on a C57BL/6 background (Berman, Westbrook et al. 2000) in order to express YFP within the neurons. Amyloid plaques are stained with anti-amyloid beta primary antibody and revealed with red Alexafluor 568. **(A)** Dystrophic neurons, as indicated by the white arrows, co-localised with an Aβ plaque. The opposite was true in regard to plaques, which commonly occurred with no dystrophy present, as indicated by the white arrow in **(B)**.

Additionally, previous studies indicate that plaque formation may occur at differing rates dependent upon cortex region (Lim, Yang et al. 2000). The cortex was thus divided into three equal sections noted as the posterior, mid and anterior regions, for the purpose of assessing plaque localisation. The distribution of plaques varied even between mice of the same gender and medication group, though as shown in figure eight the average results of the full group typically showed the same trends regardless of brain area. Female mice consistently had more plaques than males and males showed the same trend towards an increase in plaques following treatment with FK866/NA in all regions.

A



B

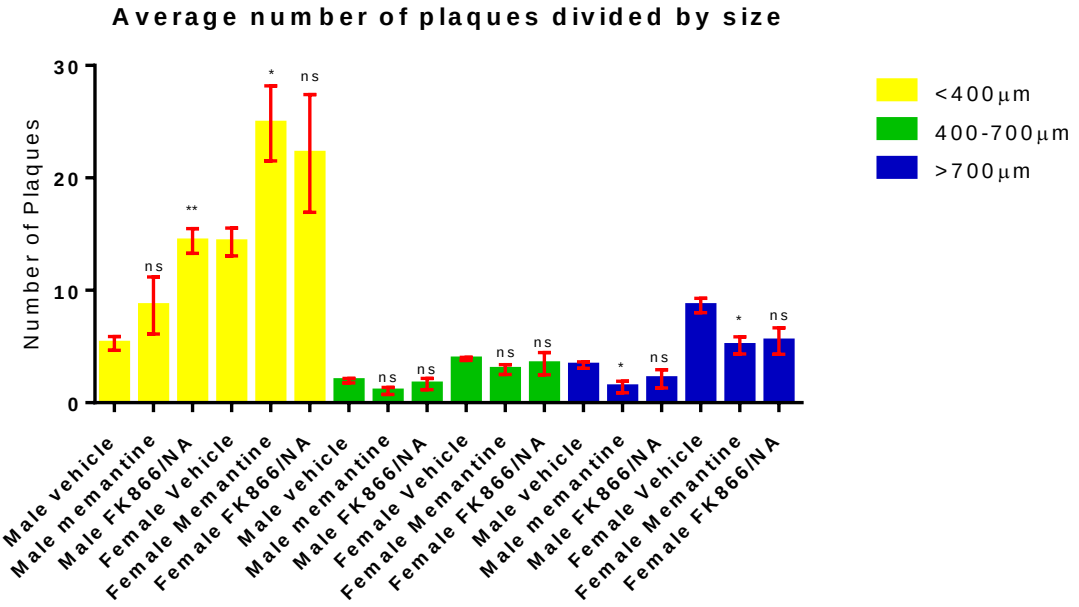
Mouse group (compared to corresponding vehicle group)	P value (via unpaired t test)
Anterior male memantine	0.2055
Anterior male FK866/NA	0.0168
Anterior female memantine	0.8024
Anterior female FK866/NA	0.9140
Mid male memantine	0.8272
Mid male FK866/NA	0.0236
Mid female memantine	0.2888
Mid female FK866/NA	0.7402
Posterior male memantine	0.8011
Posterior male FK866/NA	0.0854
Posterior female memantine	0.6147
Posterior female FK866/NA	0.9125

Figure 8 average plaque count per cortex region
(A) Results of the amyloid plaque quantification were divided into three cortex regions, again, results were obtained via confocal microscopy using a 10x air objective and quantified manually via Zen lite. Mean ±S.E.M., n=4, statistical analysis performed using unpaired t-test with Welch's correction. ns P>0.05, *P<0.05, **P<0.01, ***P<0.001, ****P<0.0001, compared with vehicle treated
(B) Statistical analysis results corresponding to the graph

3.2 Both treatment groups were shown to have reduced plaque sizes compared to the vehicle control group

The measurements of plaque area used criteria for analysis of plaque sizes from Bolmont *et al*, (small<400μm, medium 401-700μm, large>700μm), plaques were measured manually using ImageJ and quantified using these criteria. The graph shown in figure nine displays that there was a statistically significant change in the smallest plaque size group, with an increase shown in male FK866/NA ($p=0.0010$) and female memantine (0.0442) treatment groups. Medium sized plaques between 401μm and 700μm remain unchanged throughout treatment groups. Memantine was shown to reduce the quantity of the largest plaque group by a statistically significant amount in both males and females, FK866/NA also showed a reduction in both gender groups though not to a significant degree.

A



B

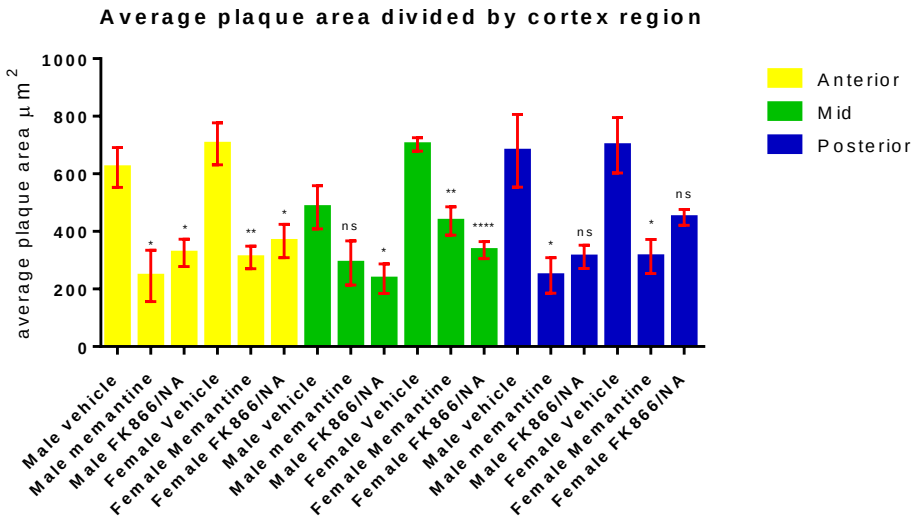
Mouse group (compared to corresponding vehicle group)	P value (via unpaired t test)
<400 male memantine	0.2778
<400 male FK866/NA	0.0010
<400 female memantine	0.0442
<400 female FK866/NA	0.2309
401-700 male memantine	0.0563
401-700 male FK866/NA	0.6139
401-700 female memantine	0.1181
401-700 female FK866/NA	0.6999
>700 male memantine	0.0246
>700 male FK866/NA	0.2383
>700 female memantine	0.0129
>700 female FK866/NA	0.0679

Figure 9. Plaque size groupings
(A) Plaque sizes quantified and calculated according to criteria established in (Bolmont, Haiss et al. 2008), graph presented as mean ±S.E.M., n=4, statistical analysis performed using unpaired t-test with Welch's correction. ns P>0.05, *P<0.05, **P<0.01, ***P<0.001, ****P<0.0001, compared with vehicle treated.
(B) P values corresponding to the graph.

3.3 Average plaque area was found to be reduced in both treatment groups

Brain section images were again quantified according to criteria used previously (Meyer-Luehmann, Spires-Jones et al. 2008) (Lim, Chu et al. 2001), for this purpose the measurements were repeated using ImageJ to calculate the average plaque area. The division of anterior, mid and posterior regions of the cortex was used (see figure 10A), consistent with the results of the plaque quantification there was no significant deviation between cortex region. The average of the three regions was taken to give an overall average plaque size for the cortex as a whole (see figure 10CInterestingly and contrary to plaque quantification, plaque area was relatively consistent between males and females. Memantine showed a reduction in plaque area of 47% in males and 50% in females (P=<0.0001 in both) compared to the vehicle group. FK866/NA shows a similar decrease in plaque area to memantine, with males showing a reduction of 48% (P=0.0001) and females reduced by 54% (P=<0.0001) though it is worth noting the data from section 3.2 indicated a large increase in plaques of the smallest group size, thus through a combination of more small plaques and a slight decrease in the largest plaques the average plaque area has been reduced.

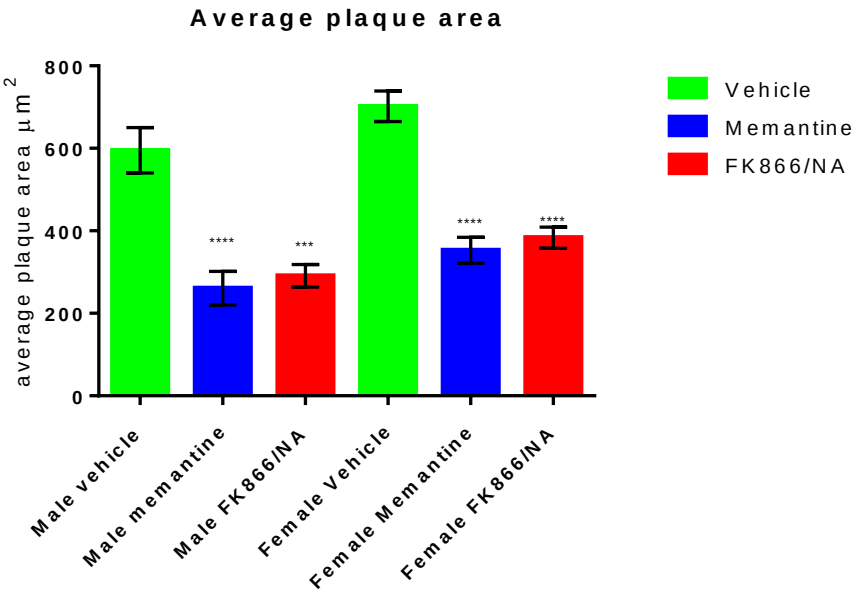
A



B

Mouse group (compared to corresponding vehicle group)	P value (via unpaired t test)
Anterior male memantine	0.0173
Anterior male FK866/NA	0.0153
Anterior female memantine	0.0063
Anterior female FK866/NA	0.0121
Mid male memantine	0.1216
Mid male FK866/NA	0.0389
Mid female memantine	0.0069
Mid female FK866/NA	<0.0001
Posterior male memantine	0.0328
Posterior male FK866/NA	0.0559
Posterior female memantine	0.0188
Posterior female FK866/NA	0.0756

C



D

Mouse group (compared to corresponding vehicle group)	P value (via unpaired t test)
Male memantine	<0.0001
Male FK866/NA	0.0001
Female memantine	<0.0001
Female FK866/NA	<0.0001

Figure 10 Average plaque areas
(A) Plaque area was calculated manually using ImageJ, averages were then calculated for each of the 5 sagittal sections before adding data to Graphpad Prism. Posterior, mid and anterior divisions were maintained as outlined in figure 8 mean ±S.E.M., n=4, statistical analysis performed using unpaired t-test with Welch's correction. ns P>0.05, *P<0.05, **P<0.01, ***P<0.001, ****P<0.0001, compared with vehicle treated. **(B)** P values corresponding to figure 10A
(C) Measurements were taken as in 10A and an average was taken of the three sections in each mouse before creating the graph. Statistical analysis was performed as in figure 10A
(D) Statistical analysis results corresponding to figure 10.

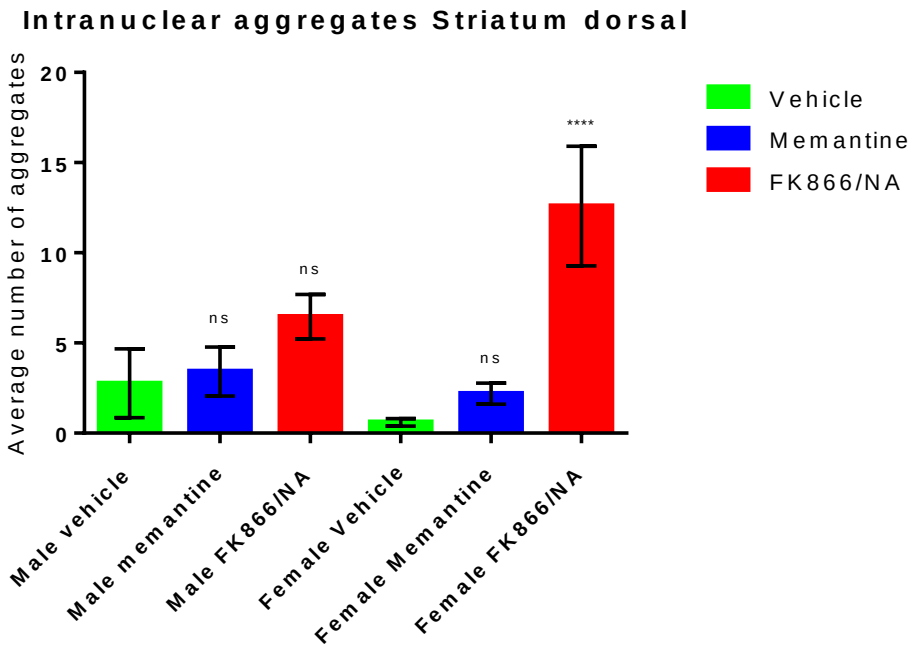
3.4 FK866/NA was shown to increase the rate of formation of nuclear aggregates of mHtt

The intention in regards to the study of nuclear aggregates of huntingtin was both to expand upon previous work conducted by the lab, in the PhD study of (Marangoni, Adalbert et al. 2014) it was found that axonal swellings occur within the stria terminalis before neuronal damage occurs, building on this it was found in the PhD study of (O.Othman) that mice treated with FK866/NA and memantine showed a reduced number of axonal swellings compared to vehicle treated mice. My study aims to investigate this further by assessing whether the medications showed any effect in regards to the pathological hallmark of Huntington's disease, the nuclear aggregates of mutant huntingtin. Vehicle treated mice would thus act as both the negative control for the medication groups as well as a group in which to study the rate of onset of nuclear inclusions independent of any effects of medication. In the same manner as the Aβ plaque study the analysis was performed in blind.

At six months the vehicle treated group had a very low number of nuclear inclusion bodies, with male vehicle treated mice having slightly more nuclear inclusions than female littermates. Memantine showed no significant change to the number of nuclear inclusions in either gender, though did show a slight, but insignificant ($P=0.4146$, Figure 11) decrease in NIIs in the striatum ventral in male mice. The results for FK866/NA indicate a large increase in nuclear aggregation, though interestingly this effect seems conserved within the female mice, with a P value of <0.0001 in both the striatum dorsal and ventral. In male mice there was a slight increase in nuclear aggregation in the striatum dorsal, though not to a significant degree and not to a comparable level of the female mice.

In contrast cytoplasmic aggregation was unaffected in the female group, with no significant deviation from the vehicle treated control group in neither the striatum dorsal or ventral, implying an increase in nuclear aggregation without a corresponding decrease in the levels of cytoplasmic mHtt. In the male group cytoplasmic aggregation was reduced in both the memantine and FK866/NA group ($P=0.0017$ and $P=0.0027$ respectively) in the striatum dorsal, with no significant changes compared to the vehicle group in the striatum ventral.

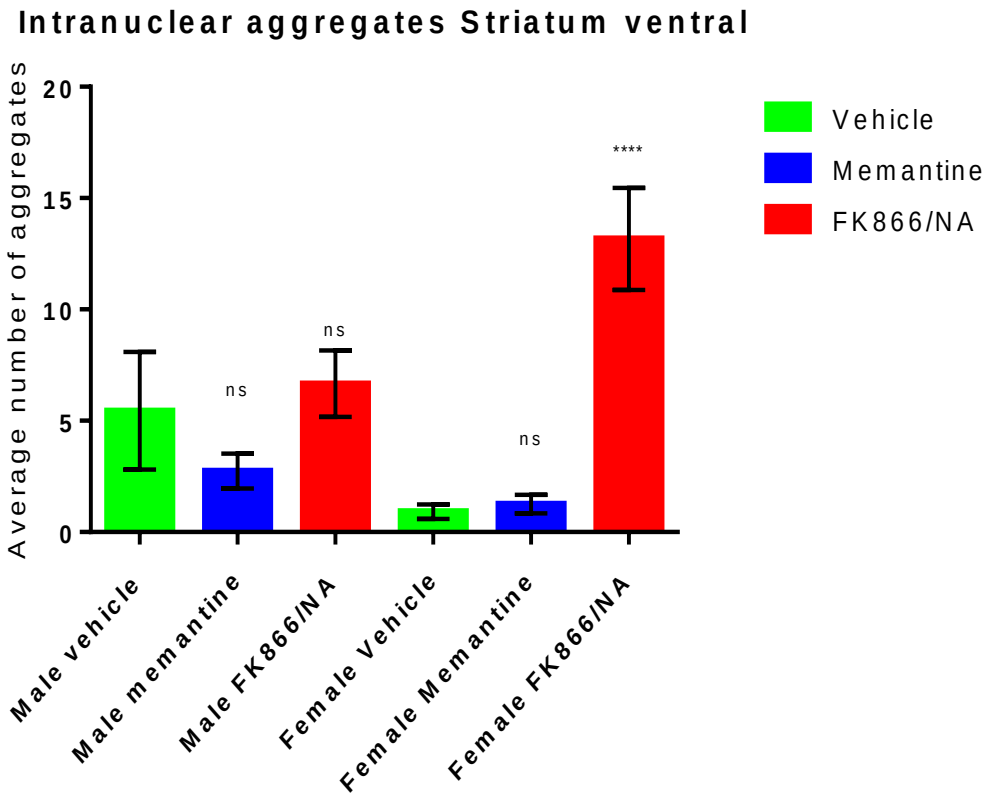
A



B

Mouse group (compared to corresponding vehicle group)	P value (via unpaired t test)
male memantine	0.9349
male FK866/NA	0.1629
female memantine	0.5502
female FK866/NA	<0.0001

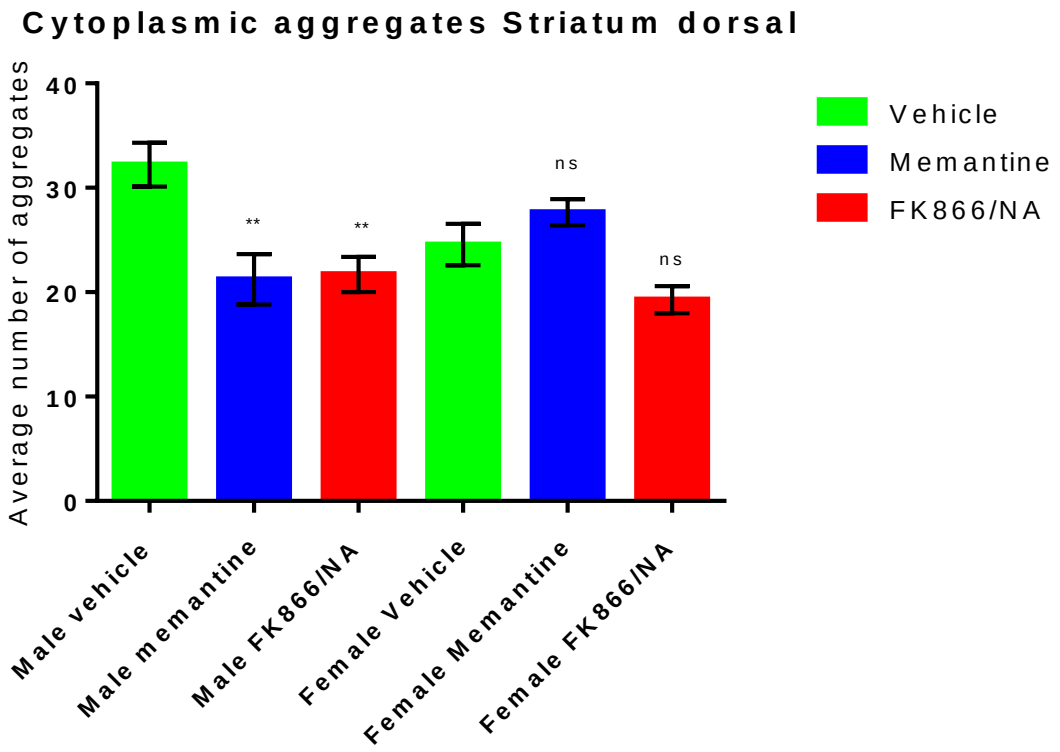
C



D

Mouse group (compared to corresponding vehicle group)	P value (via unpaired t test)
male memantine	0.4146
male FK866/NA	0.8245
female memantine	0.9457
female FK866/NA	<0.0001

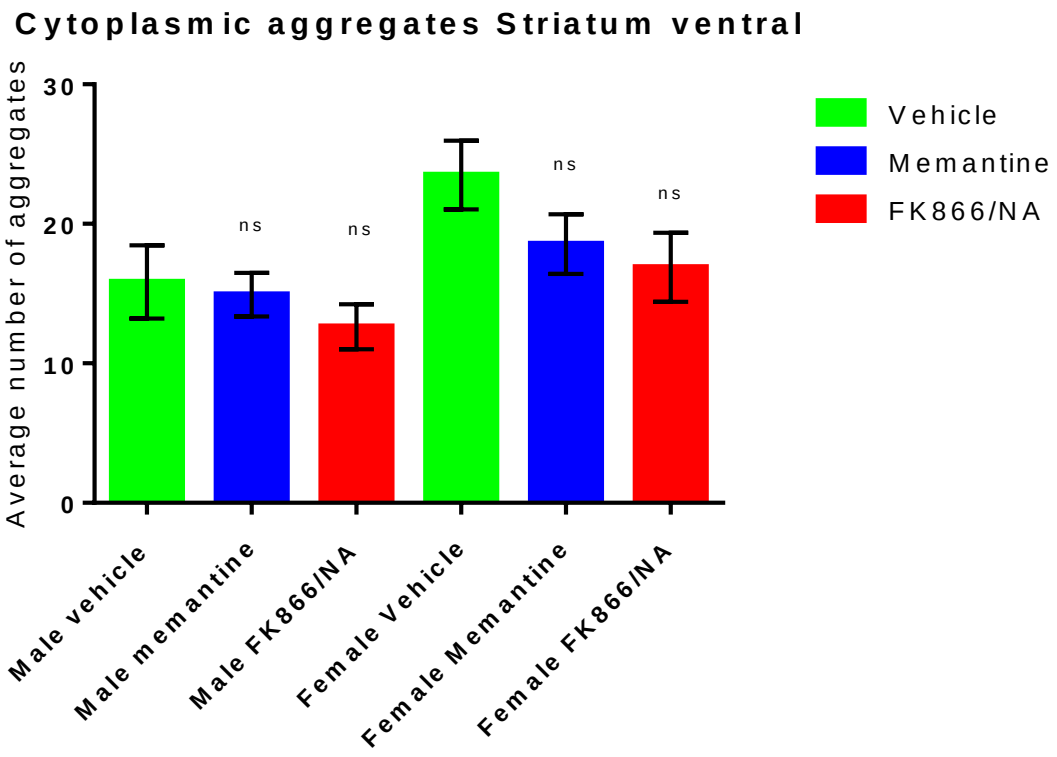
E



F

Mouse group (compared to corresponding vehicle group)	P value (via unpaired t test)
male memantine	0.0017
male FK866/NA	0.0027
female memantine	0.3135
female FK866/NA	0.0905

G



H

Mouse group (compared to corresponding vehicle group)	P value (via unpaired t test)
male memantine	0.9239
male FK866/NA	0.4043
female memantine	0.2293
female FK866/NA	0.1376

Figure 11 mHtt aggregation
(A/C/E/G) Images were acquired via confocal microscopy using a 63x oil objective, z stack images were taken consisting of 10 stacks across a 10µm depth in order to recreate 3D images which were manually rotated to analyse whether mHtt aggregates were nuclear/cytoplasmic. The aggregates were quantified from both the

striatum dorsal and striatum ventral (3 images in each area, from 3 planes in each mouse) for both nuclear and cytoplasmic aggregates as well as nuclei with no sign of aggregates. **(B/D/F/H)** Statistical analysis results corresponding to the graph (mean ±S.E.M., n=3, statistical analysis performed using unpaired t-tests. ns P>0.05, *P<0.05, **P<0.01, ***P<0.001, ****P<0.0001, compared with vehicle treated).

3.5 Pull down assay results of NMNAT2 and Htt show no evidence of a direct bind

Previous studies have shown that both NMNAT2 and Htt localise to golgi derived structures within the axon, the intention of my study was to further investigate the interaction of these two proteins, and to determine whether the proteins bound directly.

I used GST tagged NMNAT2 and Htt to perform a pull down assay following the protocols detailed in the methods section. Using multiple sets of samples collected from the same pull down assay I performed western blots using both an anti-histidine antibody as well as an anti-Htt antibody. The first western blot developed (Figure 12A) utilised the anti-histidine antibody, clearly shows an overexpression of Htt as an endogenous protein would be unlikely to be present in this amount, the band is however slightly higher than the expected 92kDa. Initially thought of as a potential positive result as a band is present in the NMNAT2 + Htt beads lane, the result was investigated further by a second western blot tagged with an anti-Htt antibody, shown in Figure 12B this result again shows a high level of expression of Htt, with bands present in the whole cell extract and pull down flow through but no sign of a band in the bead samples indicating that all traces of Htt were removed before the bead samples taken, thus making a bind between NMNAT2 and Htt unlinkely.

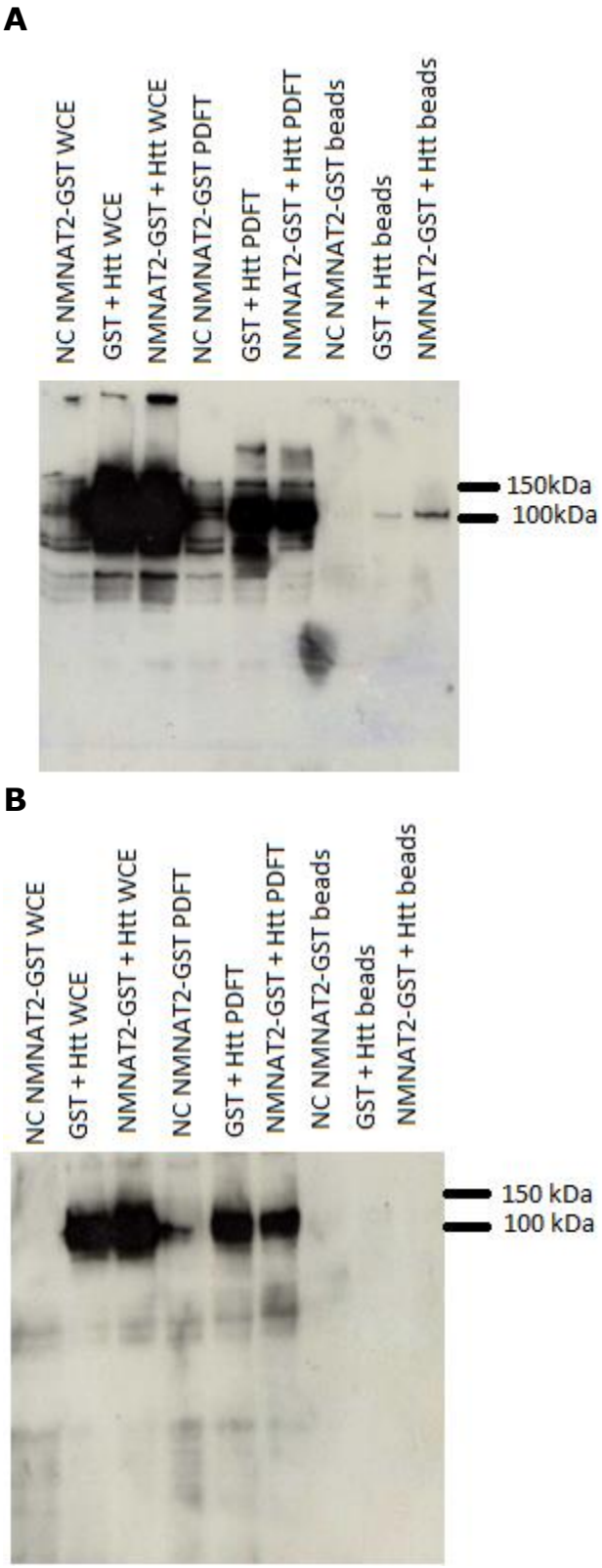


Figure 12 Pull down assay analysis

(A) Western blot resulting from the pull down assay between NMNAT2-GST and HTT-Q23, NMNAT2-GSt was expressed in BL21 *E.coli* cells and passed over Glutathione sepharose beads, HTT-Q23

was transfected via plasmid vector into HEK293T cells before being passed over the beads and allowed time to attach. Samples of the WCE as well as the PDFT were taken along with the beads themselves and used for the SDS-PAGE and western blot. The western blot was incubated with an anti-polyhistidine primary antibody along with anti-mouse IgG peroxidase secondary. **(B)** The nitrocellulose film from 12A was washed multiple times in PBS and incubated a secondary time in anti-Huntingtin primary antibody, again with anti-mouse IgG peroxidase as the secondary.

3.6 Co-immunoprecipitation confirms no direct bind occurs between NMNAT2 and Htt

I also explored the potential binding of NMNAT2 with using co-immunoprecipitation. To this purpose co-transfected HEK293T cells with plasmids encoding for NMNAT2-Flag and HTT were utilised. Following transfection the HEK cells were incubated with ANTI-Flag beads while rotating to allow maximum exposure to the beads for several hours, in a similar manner to the pull down assay samples were taken throughout the experiment for use in the SDS-PAGE and western blot as stated in materials and methods. Results of the western blot (Fig 13) indicate that Huntingtin expression levels were high, with bands corresponding to the molecular weight of the Htt construct (92kDa) appearing in both the whole cell extract as well as the pull down flow through (PDFT) in all but the negative control. In the same manner as the pull down assay after the flow through was extracted the beads were washed in PBS three times, there are no bands present in the sample of the beads for any of the three groups, thus all traces of Htt were removed during the washing process or as shown by the blot, before this in the PDFT, indicating a bind between our construct of Htt and NMNAT2 is unlikely.

A

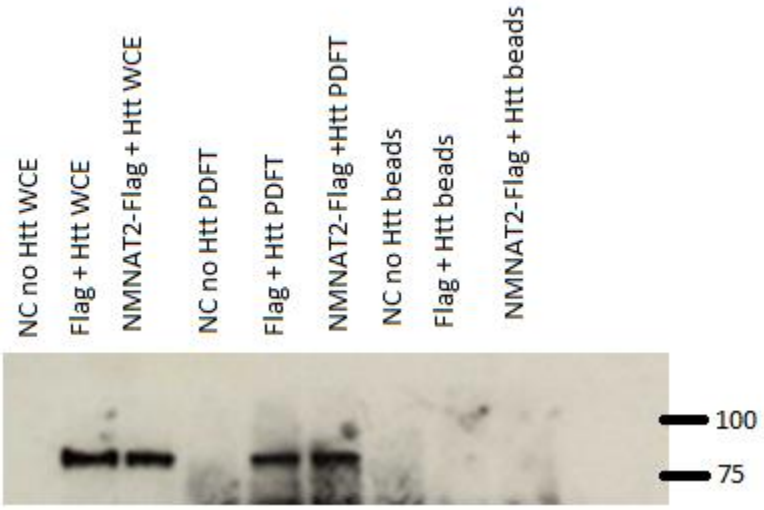
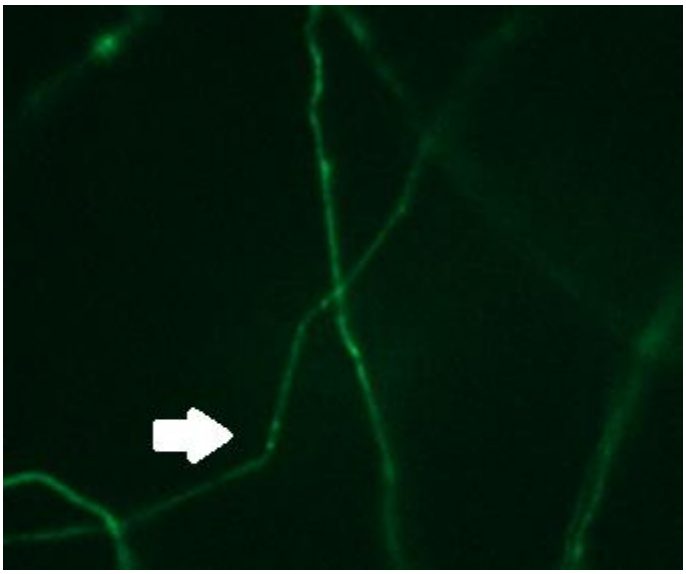


Figure 13 Co-immunoprecipitation analysis
Resulting western blot of a Co-Immunoprecipitation of NMNAT2-Flag and Htt probed with Monoclonal anti-HTT (Fisher Scientific, cat number mab2166). Bands present in lanes 2,3,5 and 6 indicate the presence of Htt (MW: 92kDa), bands occur in both the whole cell extract and the pull down flow through but not on the beads indicating that Htt did not bind the NMNAT2 attached to the Flag resin and so washed away before the samples of the beads were taken.

3.7 NMNAT2 and Htt found to be transported separately along the axon

I used SCG cells extracted from mouse pups for use in microinjections of both NMNAT2 and Htt, utilising the protocol stated in the materials and methods section the SCG cells were injected with both plasmids and allowed to incubate for 24 hours prior to analysis by TIRF microscope. Figure 14 illustrates GFP tagged NMNAT2 transported along the axon as indicated by the white arrows, though due to the overexpression of Htt-mCherry it is unclear as to whether the two proteins co-localise. A live cell recording was taken found in supplementary material 1 (video provided on disk) which better illustrates this point, Htt expression levels were low, though NMNAT2 can clearly be seen transported independently along the axon with no visible corresponding rise in Htt concentration in co-localisation.

A



B

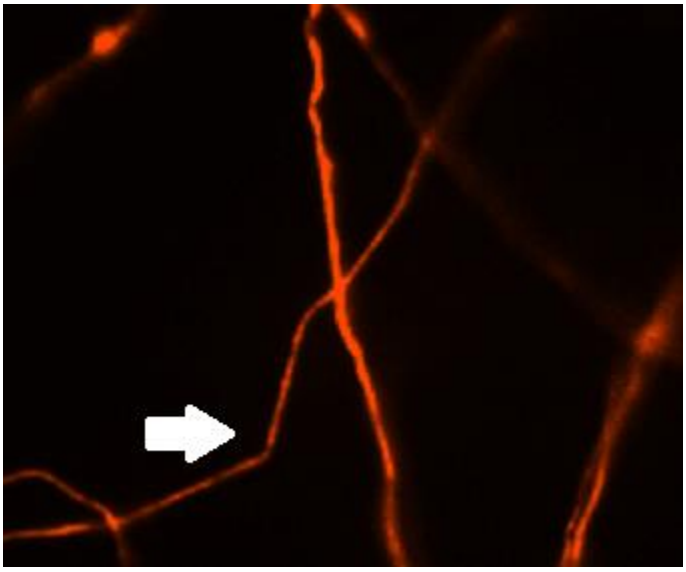


Figure 14 Microscopy results of axonal transport of NMNAT2 and Htt

(A/B) Both images taken via confocal microscope using a 20x air objective, **(A)** NMNAT2-GFP is shown in the top left of the image to be at a higher concentration within what appears to be an axonal swelling, also as indicated by the white arrow NMNAT2 is clearly shown during transport along the axon. In **(B)** Htt-mCherry is shown to be overexpressed, and present along the entirety of the axon, though no obvious co-localisation is apparent with the two instances of NMNAT2 transport as shown by the white arrow in **(A)**.

4 Discussion

The primary focus of the study has been the utilisation of FK866, an inhibitor of the synthesis of the NAD-precursor molecule NMN, previously noted for its ability to delay axon degeneration following an acute injury (Conforti, Gilley et al. 2014) within the context of both AD and HD disease models. Previous results by the lab (O.Othman, unpublished thesis 2015) had shown both a co-localisation between dystrophies and amyloid plaques, as well as a reduction in dystrophy count following treatment with both FK866/NA and memantine. This reduction was far more apparent in females than in males though this may be due to the larger number of plaques occurring in female mice. Alongside this, studies by (Marangoni, Adalbert et al. 2014) indicated axonal swellings precede neuronal damage, which was built upon by the study by O.Othman with the finding that FK866/NA reduced the number of axonal swellings in the Q140 HD model mouse. My study has further expended on these data by assessing the impact FK866/NA has on the formation of amyloid plaques in an AD model, as well as its effect on the formation of nuclear inclusion bodies of mHtt.

4.1 Medications were found to have no effect on plaque count, average plaque size was found to be reduced

The original hypothesis was that the reduction in dystrophy count following the application of either memantine or FK866/NA would coincide with a reduction in plaque count, this was based upon the observation that dystrophies would always co-localise with a plaque, though the reverse was not true, plaques would not always have a corresponding dystrophy. This observation is reinforced by previous studies (Meyer-Luehmann, Spires-Jones et al. 2008) that propose a model that would indicate plaque formation leads to neuronal cytoskeletal displacement which leads to the formation of dystrophies.

My initial quantification of the plaques however indicates that the number of plaques showed no statistically significant reduction following treatment with either medication. It was however found that in the memantine treated mice there was a noticeable lack of large plaques, a second analysis of the images for plaque size uncovered that in both memantine and FK866/NA treated mice the average plaque size had been reduced by around 50%. Analysis of the plaque sizes according to criteria used by (Bolmont, Haiss et al. 2008) demonstrated a rise (statistically significant only in male FK866/NA and female memantine) in smaller plaques across all groups, coinciding with a reduction (significant only in memantine treated mice) in large plaques. Worth noting is that all plaques above 700μm were classified as being large according to the criteria, in vehicle treated mice plaques occurred often in excess of 2000μm, whereas in memantine treated mice the large plaques rarely exceeded 1000μm. Through a combination of the reduction of large plaques alongside the increase in smaller plaques the 50% decrease in average plaque size is accounted for. In FK866/NA treated mice the overall number of plaques was higher compared to both memantine and vehicle groups and following Bolmont's criteria for plaque size classification it was shown that a the number of large plaques was reduced, to a comparable degree to memantine treated mice, though higher variability seen throughout my studies of the FK866/NA treated group the result was found to be not significant, it is worth noting that similarly to memantine the plaques found in FK866/NA mice rarely exceeded 1000μm. The increase in plaque number found in FK866/NA treated mice appears to be limited to the smallest group of plaques, this may account for the reduction in dystrophy count in both medications despite no corresponding increase in the number of plaques, (Meyer-Luehmann, Spires-Jones et al. 2008) suggests that dystrophy formation is attributed to cytoskeletal displacement occurring from plaque growth, as plaque size is restricted by both medications it

may be the case that the effects of cytoskeletal displacement is lessened and so dystrophy formation is reduced.

A further question raised would be whether the medications are limiting the growth of plaques, or enhancing the rate at which plaques are degraded. These data would suggest that growth of plaques has been limited, as it would be expected that if a plaque had grown beyond what was observed in the images, cytoskeletal alterations could have potentially already occurred leading to the formation of a dystrophy. If following this the plaque size was reduced or the plaque degraded then dystrophies would be observed with no corresponding plaque. As previously stated this was never observed, thus it is likely the case that plaque formation has been inhibited. For memantine previous studies may be applicable, following a finding that memantine reduces cortical membrane bound APP, and thus potentially reducing levels of Aβ (Unger, Svedberg et al. 2006). Theoretically with a reduced amount of soluble Aβ the formation of plaques would also be reduced as soluble and aggregated Aβ are stated to exist in a dynamic equilibrium. For FK866/NA the mechanism behind the reduced plaque size remains debateable, with few studies into the function of FK866 outside of its role as an inhibitor of NAMPT. It may be the case that through FK866's documented role as an anti-inflammatory (Busso, Karababa et al. 2008) the impact of amyloid plaques on the formation of dystrophies has been reduced.

4.2 No direct correlation was found between dystrophies and plaque count

In contrast to my hypothesis the plaque count was not reduced in correlation with the number of dystrophies in either medication group. Plaques have been implicated in previous studies (Meyer-Luehmann, Spires-Jones et al. 2008) to be the causative factor leading to dystrophy formation. The results in regards to this comparison are therefore conflicted, both memantine and FK866/NA were found to reduce the number of dystrophies, with FK866/NA appearing to be the more effective of the two. Memantine treated mice were found to have a similar number of plaques as the vehicle control group, while the FK866/NA group curiously displayed a rise in the number of plaques. As stated previously the mechanism behind the reduction in dystrophy count following treatment by memantine may be the reduced amount of soluble Aβ leading to inhibition of plaque growth, however this mechanism cannot be implicated in the FK866/NA treated mice. The previous study by (Di Stefano, Nascimento-Ferreira et al. 2015) has shown that FK866 reduces the accumulation of NMN after an acute injury, it may be possible that the cytoskeletal rearrangement as a consequence of the plaques impairs axonal transport, thus leading to an accumulation of NMN in a similar manner as the axonal injury demonstrated within the previous study. As the effects of FK866 are not yet well documented outside of its role as an inhibitor of NAMPT (Hasmann and Schemainda 2003) this is speculative, but due to its seemingly protective effect in an AD model despite the increase in plaque count, further study is warranted.

4.3 Consistent differences were found between male and female mice in the AD model

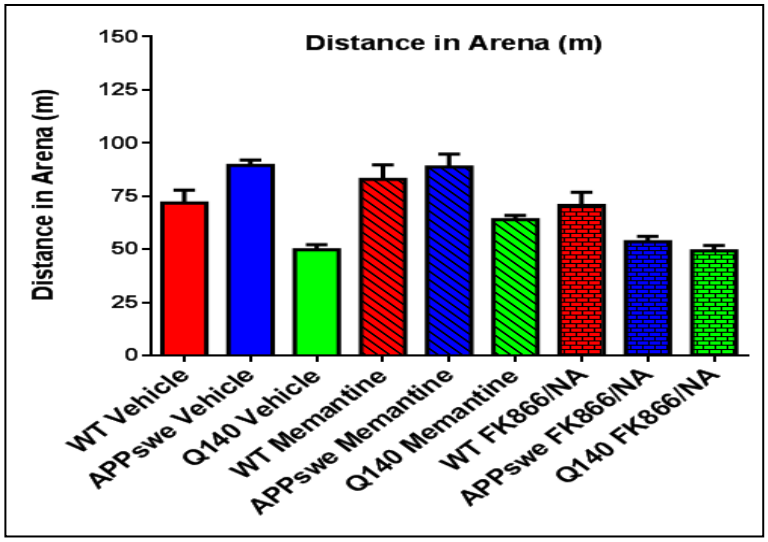
Throughout both my own work and in the literature there has been a consistent difference in the results between males and females in regards to AD. This difference was evident in the results of the plaque quantification in the cortex, with a similar difference between males and females of 10 and 38 respectively (in the vehicle treated group) with a similar difference observed previously in dystrophy counts. There is no obvious explanation to account for this difference, consistent with that reported in the disease pathology in humans. Other studies (Hirata-Fukae, Li et al. 2008) (Brookmeyer, Gray et al. 1998) have also found females to have more aggressive Aβ pathology. An increase in Aβ production coinciding with decreased activity in enzymes such as neprilysin involved (Iwata, Tsubuki et al. 2001) in the breakdown of Aβ is one of the possible mechanisms to explain this gender effect. However the differences in neprilysin levels in humans typically only occurs at an advanced age, thus any inconsistencies in the mouse model would be unlikely to occur at only 6 months. It would also be very unlikely that the differences would occur due to the mutated APP protein as the same mutation is present in both genders.

Another potential cause may be the presence of higher levels of β-secretase found in females in some transgenic model mice (Hirata-Fukae, Li et al. 2008), this causes a higher proportion of the Aβ generated to be the more pathogenic Aβ-42, which has been shown to have a higher rate of plaque formation compared to Aβ-40. The paper by Hirata-Fukae also indicates that the greatest difference between males and females in regards to β-secretase levels occurs earlier in the lifespan of the mouse, as opposed to the differences in neprilysin levels which occur typically during old age in both humans and mice. The biological basis of the difference between genders in regards to AD may be better understood through studies over a longer course of time using older mice.

4.4 FK866/NA was found to consistently increase the formation of nuclear aggregates of mHtt

In the HD model memantine treated mice showed no significant difference to the vehicle treatment group in terms of nuclear aggregates, FK866/NA produced a more interesting result, showing a general trend in which nuclear aggregation was significantly increased, with this result being far more prominent in the female mice. The toxic role of mHtt intranuclear inclusions has long been a matter of debate. Some studies support a role of intranuclear inclusions as a causative factor of the pathogenicity of HD, which could be due to the effects on transcription and issues caused within the nuclei of affected neurons (DiFiglia, Sapp et al. 1997). However other studies suggest that intranuclear aggregates represent an attempt by the cell to limit the amount of soluble mutant Huntingtin within the system (Arrasate, Mitra et al. 2004). FK866/NA treated mice seemed to show the most significant variation from the vehicle group, yet results from the behavioural studies (See fig 15) indicate that no improvements in cognition occurred in this group. Notably memantine treated mice showed a recovery in their locomotor activity to levels comparable to the WT vehicle treated group as shown by both spontaneous alternation and open field tests. This would indicate that the increase in nuclear inclusions found in the FK866/NA group does not coincide with any cognitive improvements, and would suggest that the improvements seen in cognitive tests performed on the memantine treated mice are likely via a mechanism independent of the effects on nuclear aggregates, if the benefits were due to the increase in nuclear aggregates it would be expected that these benefits were more pronounced in the FK866/NA group. A potential explanation for the improved cognitive functions in figure 15 within the memantine group compared to the Fk866/NA group may involve the regulation of synaptic and extra-synaptic activity conferred by memantine (Okamoto, Pouladi et al. 2009), with a study suggesting that mHtt increases the vulnerability of neurons to excitotoxic insult from even low levels of glutamate, and that memantine, through regulation of NMDARs confers a degree of protection against this. This would also support the theory that it is soluble mHtt, and not the aggregated form that is the major cause of pathogenicity.

A



B

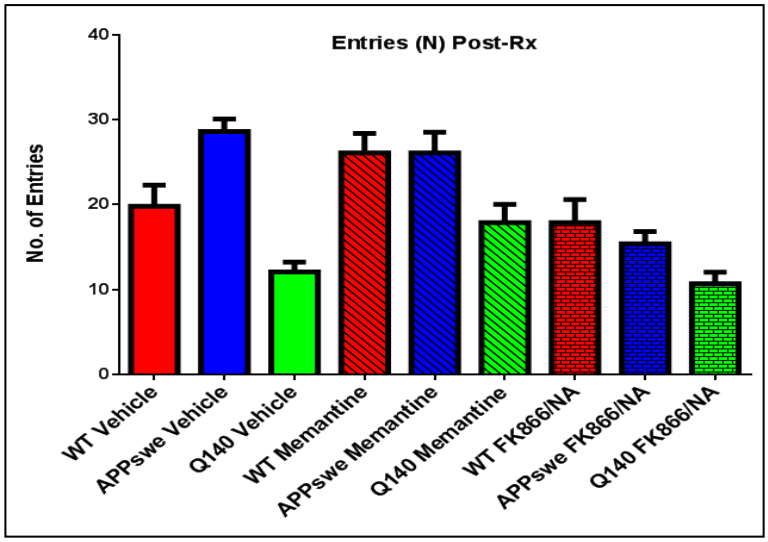


Figure 15, Behavioural studies of Q140 and APPswe mice
Results of an open field behavioural study **(A)** and a spontaneous alternation study **(B)** conducted after the application of medication previously conducted by the lab.

Data sourced from (O.Othman, unpublished PhD thesis, University of Nottingham)

The fact that FK866/NA seems to promote the formation of inclusion bodies does however present an opportunity to further study its effects in a HD model. The protective or toxic role of nuclear inclusions has commonly been studied in *in vitro* cellular models. This presents certain limitations such as a shorter period of study and the inability to assess the effect on the brain as a whole, rather than a singular cell model. With this in mind it may be the case that the formation of aggregates does indeed remove some of the soluble mHtt and so confers a protective effect, yet these models fail to take into account the downstream effects of the nuclear inclusions such as the effects upon transcription. It may be the case that these beneficial effects are temporary, and that the *in vitro* studies are conducted across a short enough time period that the downstream effects are not observed. Consistently in *in vivo* studies across multiple model organisms as well as post mortem human brains of HD patients it has been documented that these nuclear inclusion bodies contain aggregated proteins necessary for functional transcription, thus transcriptional dysregulation is a potential causative factor of cell death. As HD has a relatively slow onset with a life expectancy after diagnosis of up to 20 years *in vitro* models may not reflect properly upon the downstream effects of the formation of the nuclear inclusions. As FK866/NA has been demonstrated in this study to promote the formation of nuclear aggregates it presents an opportunity for further study. During behavioural studies it was shown that at the 6 month time point the FK866/NA group displayed little deviation in terms of cognition from the vehicle treated controls despite the increased onset of nuclear inclusions. While this does not give any indication of a protective effect it does potentially mean that at this stage there is no negative effect. This would imply that the increase in nuclear inclusions present in the FK866/NA treated mice at 6 months has not advanced HD pathology in comparison to the vehicle treated littermates, as the Q140 strain has a mild onset rate it would be of interest to study the effect of an increased number of nuclear aggregates on axonal pathology at a later point of HD onset.

This further study would be comprised of continued behavioural tests after the 6 month stage using the vehicle treated as well as FK866/NA treated mice. This would allow the onset of behavioural symptoms and cognitive decline to be observed and the long term effects of an increased rate of nuclear inclusion formation on these symptoms assessed in comparison to a vehicle treated control group in which HD pathology is already well documented.

4.5 A direct bind between NMNAT2 and Htt was found to be unlikely

Originally observed by a previous member of the lab, fluorescently labelled NMNAT2 and Htt were found to co-localise in the cell body of the neuron, with evidence from the literature supporting both proteins co-localising with golgi derived structures, this fact alone does not necessitate an interaction between the two proteins, but prior work in the lab regarding the function of NMNAT2 as a neuronal survival factor (Conforti, Gilley et al. 2014) through its scavenging of NMN warranted further investigation into a potential link. Mutant huntingtin is already established as having a role in disruption of axonal transport, an interaction between mHtt and NMNAT2 could potentially implicate the disrupted axonal transport of NMNAT2 as a cause of the build up of NMN and thus causing apoptosis.

The results of both the pull down assay and the co-immunoprecipitation were consistently negative, with no traces of Htt present in the bead samples when probed with an anti-Htt antibody despite Htt expression levels shown to be high in the WCE. This suggests a direct bind between the proteins is unlikely, but does not rule out indirect interactions such as transcriptional regulation. The conclusion to the question of whether the two proteins interact is therefore still debatable. Due to the size of the Huntingtin gene it was found to be unfeasible to transfect the full length protein via plasmid vector due to low efficiency, as such a truncated Huntingtin gene was utilised beginning at the N-terminal. It is because of this that a conclusion cannot be applied to the full length gene, the results would appear to indicate that there is no interaction between our Htt construct and NMNAT2, though the potential is still there for an interaction when using full length Huntingtin. If time constraints were not an issue it would be useful in further studies to repeat the pull down assays using additional Htt truncations to allow coverage of the entire protein, this would rule out a binding site within other regions of the protein, though this approach suffers the drawback of the possibility of conformational changes in the protein structure due to the truncation, as such the truncated fragments may still not bind even if a bind is possible with the full length protein. An alternative method would be to utilise endogenous Huntingtin, the levels of protein present would be far lower than the overexpressed exogenous Huntingtin constructs, but in the context of a pull down assay this can be overcome simply by using a large quantity of the sample, and increasing the incubation time of the WCE with the beads. This would allow for analysis of full length Huntingtin with only a slight deviation from the protocols already utilised, and may provide a far more conclusive result.

Analysis via microinjection would also appear to confirm the findings of the two previous experiments, with the hypothesis that if Huntingtin played a role in the axonal transport of NMNAT2 it would be likely that a co-localisation would occur during axonal transport as well as in the golgi apparatus. Despite low levels of expression it was observed in multiple axons (as shown in supplementary video) that the two proteins appear to be transported along the axon independently of each other. Consistent with the previous experiments these data indicate a direct bind between the two proteins is unlikely, though the potential for Htt and NMNAT2 to interact indirectly is still present. A potential future study in order to assess whether Htt fulfils a regulatory role in regards to NMNAT2 could make use of further microinjections, utilising gene silencing techniques to remove endogenous Htt while inserting either Htt or mHtt alongside NMNAT2 (all fluorescently labelled). This could allow for the study and comparison of the axonal transport of NMNAT2 and its role in neuronal survival in the context of both mHtt and Htt axons.

4.6 A potential alternative to the multiple t-test

Multiple t-tests with Welch's correction were conducted independently for the two medication groups to compare with the vehicle treated mice, though in future analysis it may be more simple to utilise a one way ANOVA test, this would allow for the parallel comparison of both medication groups against both the vehicle and each other while also accounting for the issue of type 1 errors occurring through multiple tests on the same data. Welch's correction was originally applied to circumvent the issue of having a high level of heteroscedasticity between groups, this would also be an issue in an ANOVA analysis and could once again be accounted for by using the Welch's ANOVA test.

5 Conclusions

The original hypothesis of a coinciding reduction of amyloid plaques along with dystrophies in both medication groups was determined to be false, though my data indicates that both the average plaque area, as well as the occurrence of large plaques is reduced in both treatment groups, with this effect occurring to a more significant degree in memantine. As such FK866/NA has shown to be less effective than the currently used memantine as a means of treating Alzheimer's disease. FK866/NA showed a far more interesting result upon application to the Q140 HD model, showing a consistent increase in the number of nuclear aggregates of mHtt. The role of NIIs is currently debated within the literature, this could provide the basis of future study of the effects of FK866 as well as the role of nuclear aggregates within an HD model by continued application of FK866/NA and monitoring the effects of the increased rate of NII formation at a later age when HD pathology is known to be more severe.

The results of the *in vitro* study into the possible interaction between the neuronal survival factor NMNAT2 and Huntingtin were conclusively negative, with no indication of a direct bind or colocalisation during axonal transport. This however does not rule out an indirect link between the two proteins, it is still a possibility that the axonal swellings found during HD pathology may disrupt axonal transport of NMNAT2 leading to cell death via the accumulation of NMN.

6 Acknowledgements

I would like to express my appreciation to my supervisors Laura Conforti and Marie Pardon for their assistance and guidance throughout the year as well as Othman and Andrea for their experimental assistance. I would like to thank my parents, Mandy and Ian Parry without which this masters degree would never have been possible. I would also like to thank the members of Laura Conforti's lab (Cristiano, Jessica, Simone, and Sophie) for making this year so enjoyable.

7 Appendices

Plasmids

GST (from pGEX plasmid)

MSPILGYWKIKGLVQPTRLLLEYLEEKYEEHLYERDEGDKWRNKKFELGLEF
PNLPYYIDGDVKLTQSMAIIRYIADKHNMLGGCPKERAEISMLEGAVLDIRY
GVSRIAYSKDFETLKVDFLSKLPEMLKMFEDRLCHKTYLNGDHVTHPDFML
YDALDVVLYMDPMCLDAFPKLVCFKKRIEAIPQIDKYLKSSKYIAWPLQGW
QATFGGGDHPPKSDLVPRGSPEFPGRLERPHRD
MW: 28kDa

p-GEX-NMNAT2
GST-Nmnat2 (from pGEX plasmid, Nter tagged)

MSPILGYWKIKGLVQPTRLLLEYLEEKYEEHLYERDEGDKWRNKKFELGLEF
PNLPYYIDGDVKLTQSMAIIRYIADKHNMLGGCPKERAEISMLEGAVLDIRY
GVSRIAYSKDFETLKVDFLSKLPEMLKMFEDRLCHKTYLNGDHVTHPDFML
YDALDVVLYMDPMCLDAFPKLVCFKKRIEAIPQIDKYLKSSKYIAWPLQGW
QATFGGGDHPPKSDLIEGRGIPMTETTKTHVILLACGSFNPITKGHIQMFER
ARDYLHKTGRFIVIGGIVSPVHDSYGKQGLVSSRHRLIMCQLAVQNSDWIR
VDPWECYQDTWQTTCSVLEHHRDLMKRVTGCILSNVNTPSMTPVIGQPQH
ENTQPIYQNSNVPTKPTAAKILGKVGESLSRICCVRPPVERFTFVDENANLG
TVMRYEEIELRILLLCGSDLLESFCIPGLWNEADMEVIVGDFGIVVVPRDAA
DTDRIMNHSSILRKYKNNIMVVKDDINHPMSVVSSTKSRLALQHGDGHVV
DYLSQPVIDYILKSQLYINASG
MW: 61kDa

His-mCherry-HTT(1-586; Q23) (from pcDNA plasmid, Nter tagged)

MAHHHHHHAAAAVSKGEEDNMAIIKEFMRFKVHMEGSVNGHEFEIEGEGE
GRPYEGTQTAKLKVTKGGPLPFAWDILSPQFMYGSKAYVKHPADIPDYLKL
SFPEGFKWERVMNFEDGGVVTVTQDSSLQDGEFIYKVKLRGTNFPSDGPV
MQKKTMGWEASSERMYPEDGALKGEIKQRLKLKDGGHYDAEVKTTYKAK
KPVQLPGAYNVNIKLDITSHNEDYTIVEQYERAEGRHSTGGMDELYKAAAA
TLEKLMKAFESLKSFQQQQQQQQQQQQQQQQQQQQQQQPPPPPPPPPP
QLPQPPPQAQPLLPQPQPPPPPPPPPGPAVAEEPLHRPKKELSATKKDRVN
HCLTICENIVAQSVRNSPEFQKLLGIAMELFLLCSDDAESDVRMVADECLNK
VIKALMDSNLPRLQLELYKEIKKNGAPRSLRAALWRFAELAHLVRPQKCRPY
LVNLLPCLTRTSKRPEESVQETLAAAVPKIMASFGNFANDNEIKVLLKAFIAN
LKSSSPTIRRTAAGSAVSICQHSRRTQYFYSWLLNVLLGLLVPVEDEHSTLLI
LGVLLTLRYLVPLLQQQVKDTSLKGSFGVTRKEMEVSPSAEQLVQVYELTLH
HTQHQDHNVVTGALELLQQLFRTPPPELLQTLTAVGGIGQLTAAKEESGGR
SRSGSIVELIAGGGSSCSPVLSRKQKGKVLLGEEEALEDDSESRSDVSSSA

LTASVKDEISGELAASSGVSTPGSAGHDIITEQPRSQHTLQADSVDLASCD
LTSSATDGDEEDILSHSSSQVSAVPSDPAMDLNDGTQASSPISDSSQTTTE
GPDSAVTPSDSSEIVLD
MW: 92kDa

>pCMV-Tag2B-Nmnat2

MCQLAVQNSDWIRVDPWECYQDTWQTTCSVLEHHRDLMKRVTGCILSNV
NTPSMTPVIGQPQHENTQPIYQNSNVPTKPTAAKILGKVGESLSRICCVRPP
VERFTFVDENANLGTVMRYEEIELRILLLCGSDLLESFCIPGLWNEADMEVIV
GDFGIVVVPRDAADTDRIMNHSSILRKYKNNIMVVKDDINHPMSVVSSTKS
RLALQHGDGHVVDYLSQPVIDYILKSQLYINASGLEDYKDDDDKStop

Number of amino acids: 249
Molecular weight: 28139Da (28kDa)
Theoretical pI: 5.03

8 Bibliography

Adalbert, R., et al. (2005). "A rat model of slow Wallerian degeneration (WldS) with improved preservation of neuromuscular synapses." European Journal of Neuroscience **21**(1): 271-277.

Alano, C. C., et al. (2010). "NAD(+) depletion is necessary and sufficient for PARP-1 – mediated neuronal death." The Journal of neuroscience : the official journal of the Society for Neuroscience **30**(8): 2967-2978.

Albin, R. L. and D. A. Tagle (1995). "Genetics and molecular biology of Huntington's disease." Trends in neurosciences **18**(1): 11-14.

Andrew, S. E., et al. (1993). "The relationship between trinucleotide (CAG) repeat length and clinical features of Huntington's disease." Nat Genet **4**(4): 398-403.

Arrasate, M., et al. (2004). "Inclusion body formation reduces levels of mutant huntingtin and the risk of neuronal death." Nature **431**(7010): 805-810.

Aziz, N. A., et al. (2008). "Weight loss in neurodegenerative disorders." Journal of Neurology **255**(12): 1872-1880.

Beirowski, B., et al. (2008). "The WldS gene delays axonal but not somatic degeneration in a rat glaucoma model." European Journal of Neuroscience **28**(6): 1166-1179.

Beister, A., et al. (2004). "The N-methyl-D-aspartate antagonist memantine retards progression of Huntington's disease." J Neural Transm Suppl(68): 117-122.

Berman, H. M., et al. (2000). "The Protein Data Bank." Nucleic Acids Research **28**(1): 235-242.

Blennow, K., et al. "Alzheimer's disease." The Lancet **368**(9533): 387-403.

Bolmont, T., et al. (2008). "Dynamics of the Microglial/Amyloid Interaction Indicate a Role in Plaque Maintenance." The Journal of Neuroscience **28**(16): 4283-4292.

Bonelli, R. M., et al. (2004). "Huntington's disease: present treatments and future therapeutic modalities." International clinical psychopharmacology **19**(2): 51-62.

Brookmeyer, R., et al. (1998). "Projections of Alzheimer's disease in the United States and the public health impact of delaying disease onset." American Journal of Public Health **88**(9): 1337-1342.

Browne, S. E. (2008). "Mitochondria and Huntington's Disease Pathogenesis." Annals of the New York Academy of Sciences **1147**(1): 358-382.

Browne, S. E., et al. (1997). "Oxidative damage and metabolic dysfunction in Huntington's disease: selective vulnerability of the basal ganglia." Annals of neurology **41**(5): 646-653.

Burns, A. and S. Iliffe (2009). "Alzheimer's disease." BMJ **338**.

Busso, N., et al. (2008). "Pharmacological Inhibition of Nicotinamide Phosphoribosyltransferase/Visfatin Enzymatic Activity Identifies a New Inflammatory Pathway Linked to NAD." PLoS ONE **3**(5): e2267.

Chartier-Harlin, M.-C., et al. (1991). "Early-onset Alzheimer's disease caused by mutations at codon 717 of the [beta]-amyloid precursor protein gene." Nature **353**(6347): 844-846.

Coleman, M. P., et al. (1998). "An 85-kb tandem triplication in the slow Wallerian degeneration (Wld(s)) mouse." Proceedings of the National Academy of Sciences of the United States of America **95**(17): 9985-9990.

Conforti, L., et al. (2006). "NAD+ and axon degeneration revisited: Nmnat1 cannot substitute for WldS to delay Wallerian degeneration." Cell Death Differ **14**(1): 116-127.

Danysz, W. and C. G. Parsons (2012). "Alzheimer's disease, β-amyloid, glutamate, NMDA receptors and memantine – searching for the connections." British Journal of Pharmacology **167**(2): 324-352.

de Boo, G. M., et al. (1997). "EArly cognitive and motor symptoms in identified carriers of the gene for huntington disease." Archives of Neurology **54**(11): 1353-1357.

Del Nagro, C., et al. (2014). "Depletion of the Central Metabolite NAD Leads to Oncosis-mediated Cell Death." Journal of Biological Chemistry **289**(51): 35182-35192.

Deng, Y.-P., et al. (2014). "Differential loss of thalamostriatal and corticostriatal input to striatal projection neuron types prior to overt motor symptoms in the Q140 knock-in mouse model of Huntington's disease." Frontiers in Systems Neuroscience **8**: 198.

Di Stefano, M., et al. (2015). "A rise in NAD precursor nicotinamide mononucleotide (NMN) after injury promotes axon degeneration." Cell Death Differ **22**(5): 731-742.

DiFiglia, M., et al. (1997). "Aggregation of Huntingtin in Neuronal Intranuclear Inclusions and Dystrophic Neurites in Brain." Science **277**(5334): 1990-1993.

Duara, R., et al. (1993). "A comparison of familial and sporadic Alzheimer's disease." Neurology **43**(7): 1377.

Duff, K., et al. (2007). "Psychiatric Symptoms in Huntington's Disease before Diagnosis: The Predict-HD Study." Biological Psychiatry **62**(12): 1341-1346.

Frank, S. and J. Jankovic (2010). "Advances in the Pharmacological Management of Huntington's Disease." Drugs **70**(5): 561-571.

Gatz, M., et al. (2006). "ROle of genes and environments for explaining alzheimer disease." Archives of General Psychiatry **63**(2): 168-174.

Gauthier, S., et al. (2008). "Improvement in behavioural symptoms in patients with moderate to severe Alzheimer's disease by memantine: a pooled data analysis." International Journal of Geriatric Psychiatry **23**(5): 537-545.

Geerts, H. (2009). "Of Mice and Men." CNS Drugs **23**(11): 915-926.

Gilley, J. and M. P. Coleman (2010). "Endogenous Nmnat2 Is an Essential Survival Factor for Maintenance of Healthy Axons." PLoS Biol **8**(1): e1000300.

Goedert, M., et al. (1989). "Cloning and sequencing of the cDNA encoding an isoform of microtubule-associated protein tau containing four tandem repeats: differential expression of tau protein mRNAs in human brain." The EMBO Journal **8**(2): 393-399.

Goehler, H., et al. "A Protein Interaction Network Links GIT1, an Enhancer of Huntingtin Aggregation, to Huntington's Disease." Molecular Cell **15**(6): 853-865.

Golde, T. E., et al. (2010). "Targeting Aβ and tau in Alzheimer's disease, an early interim report." Experimental neurology **223**(2): 252-266.

Goto, Y., et al. (2008). "Impaired muscarinic regulation of excitatory synaptic transmission in the APPswe/PS1dE9 mouse model of Alzheimer's disease." European Journal of Pharmacology **583**(1): 84-91.

Hasmann, M. and I. Schemainda (2003). "FK866, a Highly Specific Noncompetitive Inhibitor of Nicotinamide Phosphoribosyltransferase, Represents a Novel Mechanism for Induction of Tumor Cell Apoptosis." Cancer Research **63**(21): 7436-7442.

Hebert, L. E., et al. (1995). "AGe-specific incidence of alzheimer's disease in a community population." JAMA **273**(17): 1354-1359.

Hirata-Fukae, C., et al. (2008). "Females exhibit more extensive amyloid, but not tau, pathology in an Alzheimer transgenic model." Brain Research **1216**(0): 92-103.

Hutton, M., et al. (1998). "Association of missense and 5[prime]-splice-site mutations in tau with the inherited dementia FTDP-17." Nature **393**(6686): 702-705.

Iwata, A., et al. (2005). "Increased susceptibility of cytoplasmic over nuclear polyglutamine aggregates to autophagic degradation." Proceedings of the National Academy of Sciences of the United States of America **102**(37): 13135-13140.

Iwata, N., et al. (2001). "Metabolic Regulation of Brain Aβ by Neprilysin." Science **292**(5521): 1550-1552.

Jack, C. R., et al. (2005). "In Vivo Magnetic Resonance Microimaging of Individual Amyloid Plaques in Alzheimer's Transgenic Mice." The Journal of Neuroscience **25**(43): 10041-10048.

Jankowsky, J. L., et al. (2004). "Mutant presenilins specifically elevate the levels of the 42 residue β-amyloid peptide in vivo: evidence for augmentation of a 42-specific γ secretase." Human Molecular Genetics **13**(2): 159-170.

Jankowsky, J. L., et al. (2001). "Co-expression of multiple transgenes in mouse CNS: a comparison of strategies." Biomolecular Engineering **17**(6): 157-165.

Johnson, J. W. and S. E. Kotermanski (2006). "Mechanism of action of memantine." Current Opinion in Pharmacology **6**(1): 61-67.

Karran, E., et al. (2011). "The amyloid cascade hypothesis for Alzheimer's disease: an appraisal for the development of therapeutics." Nat Rev Drug Discov **10**(9): 698-712.

Kirkwood, S., et al. (2001). "PRogression of symptoms in the early and middle stages of huntington disease." Archives of Neurology **58**(2): 273-278.

Kokjohn, T. A. and A. E. Roher (2009). "Amyloid precursor protein transgenic mouse models and Alzheimer's disease: Understanding the paradigms, limitations and contributions." Alzheimer's & dementia : the journal of the Alzheimer's Association **5**(4): 340-347.

Kukull, W. A., et al. (1994). "Causes of Death Associated with Alzheimer Disease: Variation by Level of Cognitive Impairment Before Death." Journal of the American Geriatrics Society **42**(7): 723-726.

LaFerla, F. M. and K. N. Green (2012). "Animal Models of Alzheimer Disease." Cold Spring Harbor Perspectives in Medicine.

Lambert, J.-C., et al. (2013). "Meta-analysis of 74,046 individuals identifies 11 new susceptibility loci for Alzheimer's disease." Nature genetics **45**(12): 1452-1458.

Langbehn, D. R., et al. (2004). "A new model for prediction of the age of onset and penetrance for Huntington's disease based on CAG length." Clinical Genetics **65**(4): 267-277.

Lee, W.-C. M., et al. (2004). "Cytoplasmic aggregates trap polyglutamine-containing proteins and block axonal transport in a Drosophila model of Huntington's disease." Proceedings of the National Academy of Sciences of the United States of America **101**(9): 3224-3229.

Li, R. and M. Singh (2014). "Sex differences in cognitive impairment and Alzheimer's disease." Frontiers in Neuroendocrinology **35**(3): 385-403.

Liang, K., et al. (2010). "Estrogen Stimulates Degradation of β-Amyloid Peptide by Up-regulating Neprilysin." The Journal of Biological Chemistry **285**(2): 935-942.

Lim, G. P., et al. (2001). "The Curry Spice Curcumin Reduces Oxidative Damage and Amyloid Pathology in an Alzheimer Transgenic Mouse." The Journal of Neuroscience **21**(21): 8370-8377.

Lim, G. P., et al. (2000). "Ibuprofen Suppresses Plaque Pathology and Inflammation in a Mouse Model for Alzheimer's Disease." The Journal of Neuroscience **20**(15): 5709-5714.

Lim, J., et al. (2006). "A Protein–Protein Interaction Network for Human Inherited Ataxias and Disorders of Purkinje Cell Degeneration." Cell **125**(4): 801-814.

Ljungberg, M. C., et al. (2011). "CREB-activity and nmnat2 transcription are down-regulated prior to neurodegeneration, while NMNAT2 over-expression is neuroprotective, in a mouse model of human tauopathy." Human Molecular Genetics.

Luo, Y., et al. (2001). "Mice deficient in BACE1, the Alzheimer's [beta]-secretase, have normal phenotype and abolished [beta]-amyloid generation." Nat Neurosci **4**(3): 231-232.

Mahley, R. W., et al. (2006). "Apolipoprotein E4: A causative factor and therapeutic target in neuropathology, including Alzheimer's disease." Proceedings of the National Academy of Sciences of the United States of America **103**(15): 5644-5651.

Marangoni, M., et al. (2014). "Age-related axonal swellings precede other neuropathological hallmarks in a knock-in mouse model of Huntington's disease." Neurobiology of Aging **35**(10): 2382-2393.

McGeer, E. G. and P. L. McGeer (1976). "Duplication of biochemical changes of Huntington's chorea by intrastriatal injections of glutamic and kainic acids." Nature **263**(5577): 517-519.

Menalled, L. B. (2005). "Knock-In Mouse Models of Huntington's Disease." NeuroRx **2**(3): 465-470.

Menalled, L. B., et al. (2003). "Time course of early motor and neuropathological anomalies in a knock-in mouse model of Huntington's disease with 140 CAG repeats." The Journal of Comparative Neurology **465**(1): 11-26.

Meyer-Luehmann, M., et al. (2008). "Rapid appearance and local toxicity of amyloid-[bgr] plaques in a mouse model of Alzheimer/'s disease." Nature **451**(7179): 720-724.

Minkeviciene, R., et al. (2008). "Age-related decrease in stimulated glutamate release and vesicular glutamate transporters in APP/PS1 transgenic and wild-type mice." Journal of Neurochemistry **105**(3): 584-594.

Montoya, A., et al. (2006). "Brain imaging and cognitive dysfunctions in Huntington's disease." Journal of Psychiatry and Neuroscience **31**(1): 21-29.

Mount, C. and C. Downton (2006). "Alzheimer disease: progress or profit?" Nat Med **12**(7): 780-784.

Nance, M. A. and R. H. Myers (2001). "Juvenile onset Huntington's disease—clinical and research perspectives." Mental Retardation and Developmental Disabilities Research Reviews **7**(3): 153-157.

Newman, M., et al. (2012). "Robust homeostasis of Presenilin1 protein levels by transcript regulation." Neuroscience Letters **519**(1): 14-19.

Nistor, M., et al. (2007). "Alpha- and beta-secretase activity as a function of age and beta-amyloid in Down syndrome and normal brain." Neurobiology of Aging **28**(10): 1493-1506.

Nørremølle, A., et al. (1995). "Correlation between magnitude of CAG repeat length alterations and length of the paternal repeat in paternally inherited Huntington's disease." Clinical Genetics **47**(3): 113-117.

Nucifora, F. C., et al. (2001). "Interference by Huntingtin and Atrophin-1 with CBP-Mediated Transcription Leading to Cellular Toxicity." Science **291**(5512): 2423-2428.

Okamoto, S.-i., et al. (2009). "Balance between synaptic versus extrasynaptic NMDA receptor activity influences inclusions and neurotoxicity of mutant huntingtin." Nature medicine **15**(12): 1407-1413.

Pigino, G., et al. (2003). "Alzheimer's Presenilin 1 Mutations Impair Kinesin-Based Axonal Transport." The Journal of Neuroscience **23**(11): 4499-4508.

Pittelli, M., et al. (2010). "Inhibition of Nicotinamide Phosphoribosyltransferase: CELLULAR BIOENERGETICS REVEALS A MITOCHONDRIAL INSENSITIVE NAD POOL." Journal of Biological Chemistry **285**(44): 34106-34114.

Price, J. L., et al. (2009). "Neuropathology of Nondemented Aging: Presumptive Evidence for Preclinical Alzheimer Disease." Neurobiology of Aging **30**(7): 1026-1036.

Querfurth, H. W. and F. M. LaFerla (2010). "Alzheimer's Disease." New England Journal of Medicine **362**(4): 329-344.

Reisberg, B., et al. (2003). "Memantine in Moderate-to-Severe Alzheimer's Disease." New England Journal of Medicine **348**(14): 1333-1341.

Rising, A. C., et al. (2011). "Longitudinal Behavioral, Cross-sectional Transcriptional and Histopathological Characterization of a Knock-in Mouse Model of Huntington's Disease with 140 CAG Repeats." Experimental neurology **228**(2): 173-182.

Rocca, W. A., et al. "Sex and gender differences in the causes of dementia: A narrative review." Maturitas **79**(2): 196-201.

Rocchi, A., et al. (2003). "Causative and susceptibility genes for Alzheimer's disease: a review." Brain Research Bulletin **61**(1): 1-24.

Rodriguez, G. A., et al. (2014). "Human APOE4 increases microglia reactivity at Aβ plaques in a mouse model of Aβ deposition." Journal of Neuroinflammation **11**: 111-111.

Samsam, M., et al. (2003). "The Wld s Mutation Delays Robust Loss of Motor and Sensory Axons in a Genetic Model for Myelin-Related Axonopathy." The Journal of Neuroscience **23**(7): 2833-2839.

Saudou, F., et al. (1998). "Huntingtin Acts in the Nucleus to Induce Apoptosis but Death Does Not Correlate with the Formation of Intranuclear Inclusions." Cell **95**(1): 55-66.

Schilling, G., et al. (1999). "Intranuclear Inclusions and Neuritic Aggregates in Transgenic Mice Expressing a Mutant N-Terminal Fragment of Huntingtin." Human Molecular Genetics **8**(3): 397-407.

Schneider, L. S., et al. (2011). "LAck of evidence for the efficacy of memantine in mild alzheimer disease." Archives of Neurology **68**(8): 991-998.

Shirendeb, U. P., et al. (2012). "Mutant huntingtin's interaction with mitochondrial protein Drp1 impairs mitochondrial biogenesis and causes defective axonal transport and synaptic degeneration in Huntington's disease." Human Molecular Genetics **21**(2): 406-420.

Small, S. A. and K. Duff (2008). "Linking Aβ and Tau in Late-Onset Alzheimer's Disease: A Dual Pathway Hypothesis." Neuron **60**(4): 534-542.

Snell, R. G., et al. (1993). "Relationship between trinucleotide repeat expansion and phenotypic variation in Huntington's disease." Nat Genet **4**(4): 393-397.

Stack, E. C., et al. (2005). "Chronology of behavioral symptoms and neuropathological sequela in R6/2 Huntington's disease transgenic mice." The Journal of Comparative Neurology **490**(4): 354-370.

Stokin, G. B. and L. S. B. Goldstein (2006). "Axonal Transport and Alzheimer's Disease." Annual Review of Biochemistry **75**(1): 607-627.

Strittmatter, W. J., et al. (1993). "Apolipoprotein E: high-avidity binding to beta-amyloid and increased frequency of type 4 allele in late-onset familial Alzheimer disease." Proceedings of the National Academy of Sciences of the United States of America **90**(5): 1977-1981.

Subramaniam, S., et al. (2009). "Rhes, a Striatal Specific Protein, Mediates Mutant-Huntingtin Cytotoxicity." Science (New York, N.Y.) **324**(5932): 1327-1330.

Szapacs, M. E., et al. (2004). "Late onset loss of hippocampal 5-HT and NE is accompanied by increases in BDNF protein expression in mice co-expressing mutant APP and PS1." Neurobiology of Disease **16**(3): 572-580.

Takeda, K., et al. (2009). "Effect of Memantine on the Levels of Neuropeptides and Microglial Cells in the Brain Regions of Rats with Neuropathic Pain." Journal of Molecular Neuroscience **39**(3): 380-390.

Todd, S., et al. (2013). "Survival in dementia and predictors of mortality: a review." International Journal of Geriatric Psychiatry **28**(11): 1109-1124.

Unger, C., et al. (2006). "Effect of Subchronic Treatment of Memantine, Galantamine, and Nicotine in the Brain of Tg2576 (APPswe) Transgenic Mice." Journal of Pharmacology and Experimental Therapeutics **317**(1): 30-36.

Vos, K. J. D., et al. (2008). "Role of Axonal Transport in Neurodegenerative Diseases." Annual Review of Neuroscience **31**(1): 151-173.

Walker, F. O. "Huntington's disease." The Lancet **369**(9557): 218-228.

Williams, D. W., et al. (2000). "Tau and tau reporters disrupt central projections of sensory neurons in Drosophila." The Journal of Comparative Neurology **428**(4): 630-640.

Wu, H.-M., et al. (2009). "Novel Neuroprotective Mechanisms of Memantine: Increase in Neurotrophic Factor Release from Astroglia and Anti-Inflammation by Preventing Microglial Activation." Neuropsychopharmacology **34**(10): 2344-2357.

Wyttenbach, A., et al. (2000). "Effects of heat shock, heat shock protein 40 (HDJ-2), and proteasome inhibition on protein aggregation in cellular models of Huntington's disease." Proceedings of the National Academy of Sciences **97**(6): 2898-2903.

Xia, P., et al. (2010). "Memantine Preferentially Blocks Extrasynaptic over Synaptic NMDA Receptor Currents in Hippocampal Autapses." The Journal of Neuroscience **30**(33): 11246-11250.

Xia, P., et al. (2010). "Memantine Preferentially Blocks Extrasynaptic Over Synaptic NMDA Receptor Currents in Hippocampal Autapses." The Journal of neuroscience : the official journal of the Society for Neuroscience **30**(33): 11246-11250.

Xiao, Z.-M., et al. (2009). "Estrogen Regulation of the Neprilysin Gene Through A Hormone-Responsive Element." Journal of Molecular Neuroscience **39**(1-2): 22-26.

Yasojima, K., et al. (2001). "Reduced neprilysin in high plaque areas of Alzheimer brain: a possible relationship to deficient degradation of β-amyloid peptide." Neuroscience Letters **297**(2): 97-100.

M.Marangoni (2014) "Axon pathology in mouse models of Huntington's disease" PhD thesis. University of Nottingham

O.Othman (2015) " Neuroprotective effects of memantine and FK866/Nicotinic acid in in vivo mouse models of Alzheimer's disease (AD) and Huntington's Disease (HD)" Unpublished PhD thesis. University of Nottingham